



Contents lists available at ScienceDirect

Earth-Science Reviews

journal homepage: www.elsevier.com/locate/earscirev

The largest volcanic eruptions on Earth

Scott E. Bryan^{a,b,c,*}, Ingrid Ukstins Peate^d, David W. Peate^d, Stephen Self^e, Dougal A. Jerram^f, Michael R. Mawby^f, J.S. (Goonie) Marsh^g, Jodie A. Miller^h

^a Department of Geology & Geophysics, Yale University, PO Box 208109 New Haven CT 06520-8109, USA

^b Centre for Earth and Environmental Science Research, Kingston University, Penhryn Road, Kingston Upon Thames, Surrey KT1 2EE, United Kingdom

^c Biogeoscience, Queensland University of Technology, GPO Box 2434, Brisbane, Queensland 4001, Australia

^d Department of Geoscience, 121 Trowbridge Hall, University of Iowa, Iowa City, IA 52242, United Kingdom

^e Department of Earth Sciences, The Open University, Walton Hall, Milton Keynes MK7 6AA, United Kingdom

^f Department of Earth Sciences, University of Durham, South Road, Durham DH1 3LE, United Kingdom

^g Department of Geology, Rhodes University, PO Box 94, Grahamstown 6140, South Africa

^h Department of Geology, Stellenbosch University, Private Bag X1, Matieland, Western Cape 7602, South Africa

ARTICLE INFO

Article history:

Received 17 December 2009

Accepted 1 July 2010

Available online 21 July 2010

Keywords:

super-eruption

Large Igneous Provinces

flood basalt

rhyolite

ignimbrite

ABSTRACT

Large igneous provinces (LIPs) are sites of the most frequently recurring, largest volume basaltic and silicic eruptions in Earth history. These large-volume ($>1000 \text{ km}^3$ dense rock equivalent) and large-magnitude ($>M8$) eruptions produce areally extensive (10^4 – 10^5 km^2) basaltic lava flow fields and silicic ignimbrites that are the main building blocks of LIPs. Available information on the largest eruptive units are primarily from the Columbia River and Deccan provinces for the dimensions of flood basalt eruptions, and the Paraná–Etendeka and Afro-Arabian provinces for the silicic ignimbrite eruptions. In addition, three large-volume (675–2000 km^3) silicic lava flows have also been mapped out in the Proterozoic Gawler Range province (Australia), an interpreted LIP remnant. Magma volumes of $>1000 \text{ km}^3$ have also been emplaced as high-level basaltic and rhyolitic sills in LIPs. The data sets indicate comparable eruption magnitudes between the basaltic and silicic eruptions, but due to considerable volumes residing as co-ignimbrite ash deposits, the current volume constraints for the silicic ignimbrite eruptions may be considerably underestimated. Magma composition thus appears to be no barrier to the volume of magma emitted during an individual eruption. Despite this general similarity in magnitude, flood basaltic and silicic eruptions are very different in terms of eruption style, duration, intensity, vent configuration, and emplacement style. Flood basaltic eruptions are dominantly effusive and Hawaiian–Strombolian in style, with magma discharge rates of $\sim 10^6$ – 10^8 kg s^{-1} and eruption durations estimated at years to tens of years that emplace dominantly compound pahoehoe lava flow fields. Effusive and fissural eruptions have also emplaced some large-volume silicic lavas, but discharge rates are unknown, and may be up to an order of magnitude greater than those of flood basalt lava eruptions for emplacement to be on realistic time scales (<10 years). Most silicic eruptions, however, are moderately to highly explosive, producing co-current pyroclastic fountains (rarely Plinian) with discharge rates of 10^9 – $10^{11} \text{ kg s}^{-1}$ that emplace welded to rheomorphic ignimbrites. At present, durations for the large-magnitude silicic eruptions are unconstrained; at discharge rates of 10^9 kg s^{-1} , equivalent to the peak of the 1991 Mt Pinatubo eruption, the largest silicic eruptions would take many months to evacuate $>5000 \text{ km}^3$ of magma. The generally simple deposit structure is more suggestive of short-duration (hours to days) and high intensity ($\sim 10^{11} \text{ kg s}^{-1}$) eruptions, perhaps with hiatuses in some cases. These extreme discharge rates would be facilitated by multiple point, fissure and/or ring fracture venting of magma. Eruption frequencies are much elevated for large-magnitude eruptions of both magma types during LIP-forming episodes. However, in basalt-dominated provinces (continental and ocean basin flood basalt provinces, oceanic plateaus, volcanic rifted margins), large magnitude ($>M8$) basaltic eruptions have much shorter recurrence intervals of 10^3 – 10^4 years, whereas similar magnitude silicic eruptions may have recurrence intervals of up to 10^5 years. The Paraná–Etendeka province was the site of at least nine $>M8$ silicic eruptions over an ~ 1 Myr period at $\sim 132 \text{ Ma}$; a similar eruption frequency, although with a fewer number of silicic eruptions is also observed for the Afro-Arabian Province. The huge volumes of basaltic and silicic magma erupted in quick succession during LIP events raises several unresolved issues in terms of locus of magma generation and storage (if any) in the crust prior to eruption, and paths and rates of ascent from magma reservoirs to the surface.

* Corresponding author. Queensland University of Technology, Biogeoscience, Faculty of Science & Technology, GPO Box 2434 Brisbane, Queensland 4001 Australia. Tel.: +61 7 3138 4827; fax: +61 7 3138 2330.

E-mail addresses: scott.bryan@qut.edu.au (S.E. Bryan), ingrid-peate@uiowa.edu (I.U. Peate), david-peate@uiowa.edu (D.W. Peate), Stephen.Self@open.ac.uk (S. Self), d.a.jerram@durham.ac.uk (D.A. Jerram), m.r.mawby@durham.ac.uk (M.R. Mawby), goonie.marsh@ru.ac.za (J.S.(G.) Marsh), jmiller@sun.ac.za (J.A. Miller).

Available data indicate four end-member magma petrogenetic pathways in LIPs: 1) flood basalt magmas with primitive, mantle-dominated geochemical signatures (often high-Ti basalt magma types) that were either transferred directly from melting regions in the upper mantle to fissure vents at surface, or resided temporarily in reservoirs in the upper mantle or in mafic underplate thereby preventing extensive crustal contamination or crystallisation; 2) flood basalt magmas (often low-Ti types) that have undergone storage at lower \pm upper crustal depths resulting in crustal assimilation, crystallisation, and degassing; 3) generation of high-temperature anhydrous, crystal-poor silicic magmas (e.g., Paraná–Etendeka quartz latites) by large-scale AFC processes involving lower crustal granulite melting and/or basaltic underplate remelting; and 4) rejuvenation of upper-crustal batholiths (mainly near-solidus crystal mush) by shallow intrusion and underplating by mafic magma providing thermal and volatile input to produce large volumes of crystal-rich (30–50%) dacitic to rhyolitic magma and for ignimbrite-producing eruptions, well-defined calderas up to 80 km diameter (e.g., Fish Canyon Tuff model), and which characterise of some silicic eruptions in silicic LIPs.

© 2010 Elsevier B.V. All rights reserved.

Contents

1. Introduction	208
2. Determining the products of single eruptions	209
2.1. Volume estimations	209
3. LIP eruptions	213
3.1. Flood basalt eruptions in LIPs	213
3.2. Silicic eruptions in LIPs	215
4. Magnitude of LIP eruptions	217
5. Discussion	220
5.1. Eruption magnitudes of flood basalts vs rhyolites	221
5.2. Discharge rates	221
5.3. Frequency of large-magnitude (>M8) eruptions from LIPs	223
5.4. Generation and storage of large magnitude LIP eruptions	223
6. Conclusions	226
Acknowledgements	226
References	226

1. Introduction

The generation and emplacement of large igneous provinces (LIPs) are anomalous transient igneous events in Earth's history resulting in rapid and large volume accumulations of volcanic and intrusive igneous rock (Coffin and Eldholm, 1994; Bryan and Ernst, 2008). LIP events have been estimated to have had a frequency of one every 20 Myrs since the Archean (Ernst and Buchan, 2001), but when the current oceanic LIP record dating back to 250 Ma is also included, this frequency is reduced to one per 10 Myr (Coffin and Eldholm, 2001; see also Prokoph et al., 2004). The volcanic and intrusive products of individual LIPs collectively cover areas well in excess of 0.1 Mkm², and typically, extruded volcanic deposit volumes are ≥ 1 Mkm³. Oceanic plateaus define the upper limits of the areal and volumetric dimensions of terrestrial LIPs, with reconstruction of the Ontong-Java, Hikurangi and Manihiki plateaus (Taylor, 2006) having a pre-rift areal extent of ~ 3.5 Mkm², larger than the Indian sub-continent, a maximum crustal thickness of 30 km and a maximum igneous volume of 59–77 Mkm³ (Kerr and Mahoney, 2007).

A distinguishing feature of LIPs, as exemplified by continental flood basalt provinces, is the high magma emplacement rates (e.g., Storey et al., 2007) where aggregate magma volumes of ≥ 1 Mkm³ are emplaced from a focussed source during 1 to 5 million year-long periods or pulses (Bryan and Ernst, 2008). In detail, most LIP eruptions had magnitudes significantly greater than those of historic eruptions, tending towards extraordinarily large-volume eruptions ($>10^3$ km³; Tolan et al., 1989; Jerram, 2002; White et al., 2009; Chenet et al., 2009), making LIP volcanism exceptional. However, to produce such tremendous cumulative volumes of erupted magma, the short-lived, main eruptive pulses of LIP events must consist of many and frequently recurring, large-volume eruptions, each evacuating 10^2 – 10^3 km³ of magma. Consequently, it is the volume of magma emitted

during these individual eruptions, the frequency of such large-volume eruptions, and the total volume of magma intruded and released during the main igneous pulses that make LIP events so exceptional in Earth history, and called upon to explain environmental and climatic changes and mass extinctions (e.g., Rampino & Stothers, 1988; Courtillot, 1999; Courtillot and Renne, 2003; Wignall, 2001; 2005; Self et al., 2005; Kelley, 2007).

Despite the total cumulative erupted volumes and timing of LIP events being reasonably well-constrained (Coffin and Eldholm, 1994; Bryan and Ernst, 2008), our current understanding of the size, duration and frequency of individual LIP eruptions is very limited. Considerable focus has been on flood basalt eruptions in the continental flood basalt provinces, which are the best exposed and studied examples of LIPs. Almost all information on the size of individual flood basaltic eruptions comes from the many studies undertaken on the Columbia River Flood Basalt Province, which is the smallest (~ 0.234 Mkm³) and youngest example of a continental flood basalt province (e.g., Swanson et al., 1975; Reidel et al., 1989; Tolan et al., 1989; Self et al., 1997; Camp et al., 2003; Hooper et al., 2007). It is only recently that some understanding has been made on the magnitude of flood basalt eruptions from other flood basalt provinces (Deccan: Jay and Widdowson, 2006; Self et al., 2008; Chenet et al., 2009).

By contrast, similarly large-volume silicic volcanic eruptions are known from a number of tectonic regimes, but which are exclusively continental in crustal setting. Extension of active continental margins, whether in narrow, rifted arc or back-arc settings (e.g., Taupo Volcanic Zone) or broader extensional belts (e.g., Basin & Range Province, western USA) and intraplate to rifted continental environments (e.g., Afro-Arabian province) have been the most productive settings for large-volume (>1000 km³) silicic eruptions since the middle Tertiary (Mason et al., 2004). Consequently, unlike flood basalt eruptions,

large-volume silicic eruptions are not exclusive to LIPs and not restricted to discrete eruptive episodes such as LIP events throughout Earth history (Thordarson et al., 2009). The presently determined average recurrence rate of one silicic eruption of Magnitude 8 or greater (Pyle, 1995; 2000) every 100,000–200,000 years (Self, 2006) reflects the contribution from sources in a variety of tectonic settings. This relatively higher frequency for large magnitude silicic eruptions means that they pose a greater hazard to human civilization than flood basaltic eruptions (Thordarson et al., 2009). What is distinctive regarding large-volume silicic eruptions from LIPs is their association with large-magnitude basaltic eruptions, their enhanced frequency and the cumulative volume of silicic magma emplaced (up to 10 Mkm^3) when compared to other tectonic settings (Bryan et al., 2002; Mason et al., 2004; Bryan and Ernst, 2008).

Super-eruptions have recently been defined as those yielding more than $1 \times 10^{15} \text{ kg}$ of magma (Sparks et al., 2005; Self, 2006). For rhyolitic eruptions, this is equivalent to $\sim 410 \text{ km}^3$ (at a magma density of 2450 kg m^{-3}). However, super-eruption has not yet been strictly applied to basaltic eruptions, where only 360 km^3 of erupted magma is required, given their higher magma density of $\sim 2750 \text{ kg m}^{-3}$. Here we present a compilation of known eruption volumes for the very largest (>Magnitude 8.5, equivalent to $>1160 \text{ km}^3$ of basalt lava, or $>1280 \text{ km}^3$ of dense silicic lava or ignimbrite) basaltic and rhyolitic eruptions from LIPs. This is to complement recent compilations for example, on the largest Tertiary–Quaternary silicic explosive eruptions (Mason et al., 2004), and provide a basis for improved long-term eruption rate estimates (e.g., White et al., 2006), which are currently based on sparse data from LIPs. Consequently, our understanding of what are the largest eruptions is limited and biased to late Tertiary and Recent volcanic activity. In these recent compilations, only one silicic eruption of magnitude 9 ($1 \times 10^{16} \text{ kg}$, or $\sim 5000 \text{ km}^3$ of dense magma) has been recognized, which occurred 28 Ma (Lipman et al., 1970; Mason et al., 2004). Issues investigated with the data set presented here are: What are the largest eruptions? What are the physical limits that may exist for eruption magnitude and whether magma composition imposes any limitation? How do basaltic and silicic “super-eruptions” differ in terms of eruption mechanisms, rates, durations and frequencies during LIP-forming events? And what implications do these issues have for the generation and storage of such prodigious magma volumes?

2. Determining the products of single eruptions

Determining what deposits constitute the products of an individual eruption and assessing erupted volumes are not straightforward in LIPs given exposure problems (e.g., concealment, burial or uplift and erosion), the potential great extent of (often thin) eruptive units (10^4 – 10^6 km^2), tectonic deformation and fragmentation, and subtle lithologic or geochemical distinction. Important tools for discriminating individual eruptive units are superposition, the presence or absence of internal palaeosoils, sedimentary or other lithologically distinct deposits (Figs. 1 and 2), petrography, mineral chemistry, bulk rock or juvenile component compositional characteristics, and paleomagnetic character (see Milner et al., 1995; Self et al., 1997; Jay et al., 2009; Chenet et al., 2009). Geochemistry has been useful at regional scales in defining stratigraphic units of basaltic lavas with distinctive geochemical features (e.g., Mangan et al., 1986; Devey and Lightfoot, 1986; Peate et al., 1992; Hooper, 1997; Marsh et al., 2001) but greatest success is achieved where a combination of approaches are used (e.g., Chenet et al., 2008; 2009; Jay et al., 2009). Examples of significant regional correlations include the dissected and tectonically fragmented silicic eruptive units of the Paraná–Etendeka flood basalt province (Milner and Duncan, 1987; Milner et al., 1992; 1995) and on-land ignimbrites of the Afro-Arabian province with distal co-ignimbrite ash deposited in marine basins (Ukstins Peate et al., 2005, 2008).

A complication in unravelling the products of an individual eruption in LIPs is caused by factors such as the great areal extent of volcanism, multiple vent activity, potentially long crustal transport distances, and in particular, the duration of flood basalt eruptions. Given these factors, synchronicity of contrasting magmas (Fig. 3) and of widely separated eruptions are a distinct possibility. Because of the high frequency of large eruptions during a LIP-forming event, the products of the majority of eruptions cannot be discriminated on the basis of current radiometric dating techniques. Heterogeneous granitoids produced by mingled gabbroic and granitic magmas in associated intrusive complexes (e.g., Messum; Fig. 3A) record the simultaneous existence of mafic and silicic magmas in LIP plumbing systems (Vogel, 1982; Ewart et al., 2002). Consequently, it remains unclear where interbedded units do exist whether this interstratification implies either a substantial timebreak or simultaneous (basalt–rhyolite or basalt–basalt) eruptions from different vent regions within the province.

Two pertinent examples of the above occur in the Paraná–Etendeka flood basalt province (Fig. 4): 1) two basaltic magma types (Urubici and Gramado) are interbedded in the southern Paraná (Peate et al., 1999); and 2) two discontinuous and chemically different basalt lavas are interbedded within the Goboboseb Quartz Latite of the Etendeka Province (Milner and Ewart, 1989; Milner et al., 1992; 1995). In the Paraná example, compositionally identical Urubici-type basaltic lava flow units 9 and 10, exposed along the coastal escarpment, were divided into two units as they are separated by a Gramado-type basaltic lava flow near Urubici. We suggest that units 9 and 10 were part of a single eruptive event (sourced from a vent region to the north where Urubici-type magmas predominate) that coincided with the simultaneous eruption of a Gramado flow field from the south.

For flood basalt eruptions, the term *lava flow field* refers to the aggregate product of a single eruption and can be formed of one or more lava flows, each the product of a vent or a group of vents along a fissure segment (Self et al., 1997). Consequently, all flood basalt lava fields are compound pahoehoe lavas composed of 1000s of lava sheet lobes, and innumerable smaller lobes, stacked/superposed in some places and laterally arranged in others. By contrast, the stratigraphy of silicic eruptive units appears much simpler, as exemplified by the Paraná–Etendeka quartz latites (Fig. 5), which crop out as relatively featureless extensive sheets with a simple internal structure and jointing, leading to the interpretation as single flow or cooling units (Milner et al., 1992). A simple deposit structure, an extremely chemically uniform or distinctive character and chemical distinction from other silicic units are used here to support the interpretation of silicic units in flood basalt provinces such as the Paraná–Etendeka, Karoo and Afro-Arabian provinces as being the products of individual eruptions.

2.1. Volume estimations

Volume estimation of LIP eruptive units is a difficult task, and is strongly affected by erosion, burial and concealment of eruptive units, and tectonic fragmentation of the provinces. It requires excellent exposure, little deformation or erosion of the sequences, and textural and/or geochemical distinction to aid in correlation. As a consequence of these factors, each LIP will have a different prospectivity potential for delineating the products of large-magnitude eruptions (Table 1). For the basaltic eruptive units, long-distance crustal transport in sill-dyke complexes and multiple venting sites (e.g., Scarab Peak lavas, Ferrar LIP, Elliot et al., 1999) complicate this task. Additional complications arise for the silicic eruptive units in that nonwelded pyroclastic material is more easily eroded than massive or even autobrecciated lava, and that deposit volumes may reside as intracaldera, outflow, tephra fallout (from Plinian and/or co-ignimbrite ash plumes) deposits (Mason et al., 2004; Self, 2006; de Silva, 2009), as voluminous resedimented pyroclastic

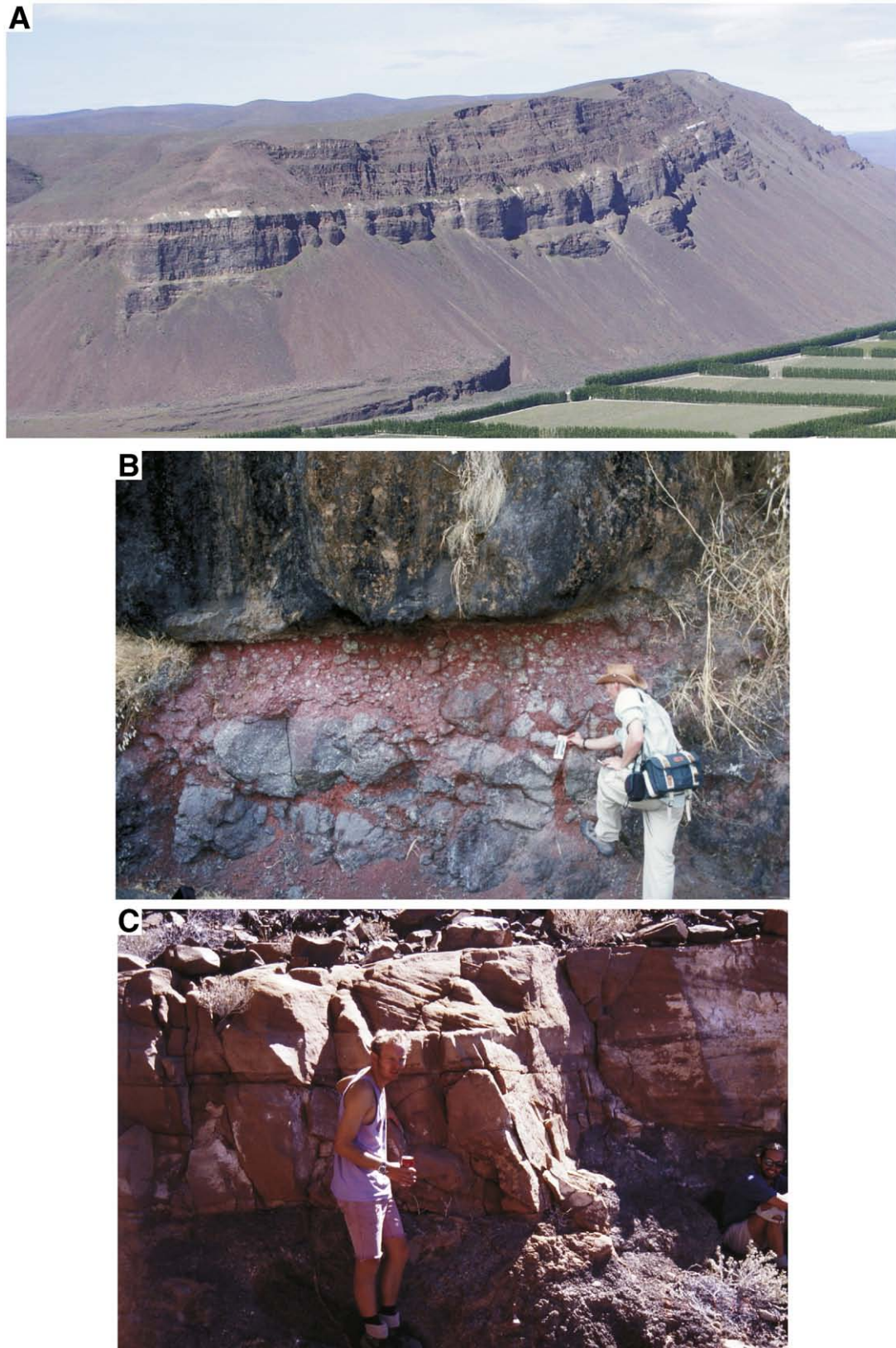


Fig. 1. Examples of intervening deposits recording time breaks between basaltic LIP eruptions. A) Gently folded Columbia River Basalt lavas exposed at Sentinel Gap ($46^{\circ} 48.750' N$ $119^{\circ} 56.910' W$), Washington, USA, showing part of the younger Wanapum Formation lavas overlying upper part of the voluminous Grande Ronde Formation lavas and separated by the Vantage sediment inter-bed (white layer, up to 20 m thick). Total height of cliff is ~300 m. B) Contact between lavas of the Ambenali Formation of the Wai Sub-group (Deccan LIP, $17^{\circ} 53.710' N$ $73^{\circ} 42.715' E$) with a massive base of the upper lava's core (note, virtually no lower crustal zone) resting on a mechanically eroded/brecciated S-type pahoehoe top of an upper crustal zone of the lower flow with relatively thick red-weathering zone of silty-clayey material between the breccia clasts. C) Aeolian cross-bedded sandstone interbedded with olivine-phyric compound pahoehoe flood basaltic lavas of the Paraná–Etendeka LIP, Huab Outliers, Namibia ($20^{\circ} 39.161' S$ $14^{\circ} 09.350' E$).

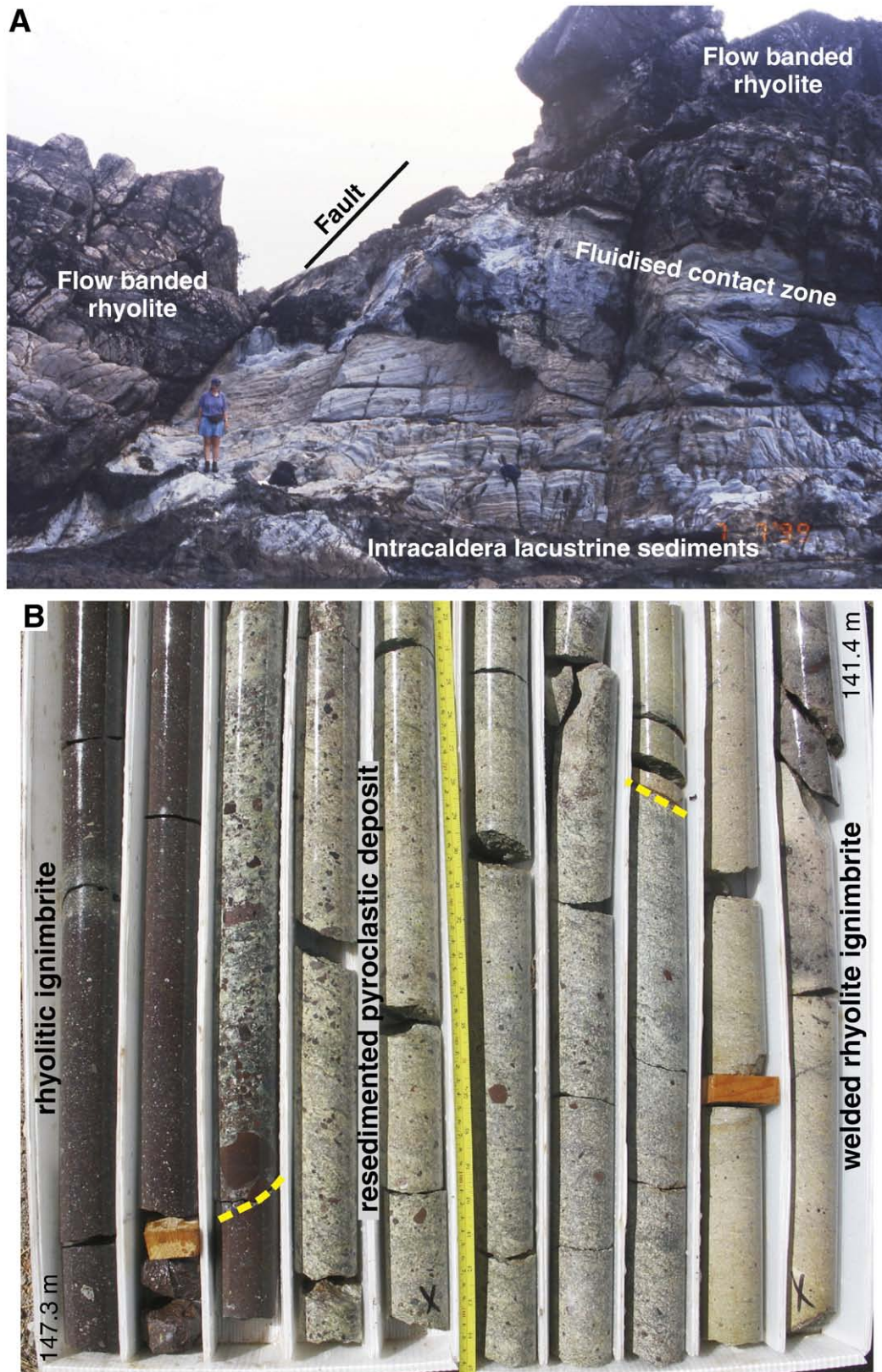


Fig. 2. Examples of intervening deposits recording time breaks between silic eruptions in LIPs. A) Intracaldera lacustrine sedimentary succession developed between two major ignimbrite and caldera-forming eruptions. This well-bedded, fine-grained, low-energy sedimentary package overlies a capping lag breccia unit to a welded rhyolitic ignimbrite, and is itself overlain by a flow banded rhyolite lava flow/dome complex with a marginal hyaloclastite and fluidised sediment contact zone; Whitsunday Island ($20^{\circ} 18.545'S$ $149^{\circ} 2.873'E$), Whitsunday silicic LIP. B) Normally graded, clast-supported and matrix-poor, resedimented pyroclastic unit overlying a reddened top to a fine-grained rhyolitic ignimbrite at left and capped by a welded, fine-grained base to a rhyolitic ignimbrite at right. Contacts marked by yellow dashed lines ($21^{\circ} 41.305' N$ $103^{\circ} 52.520' W$; San Martin de Bolaños mine, drill hole Z-425 @ 147.3–141.4 m depth; Sierra Madre Occidental silicic LIP, Mexico).

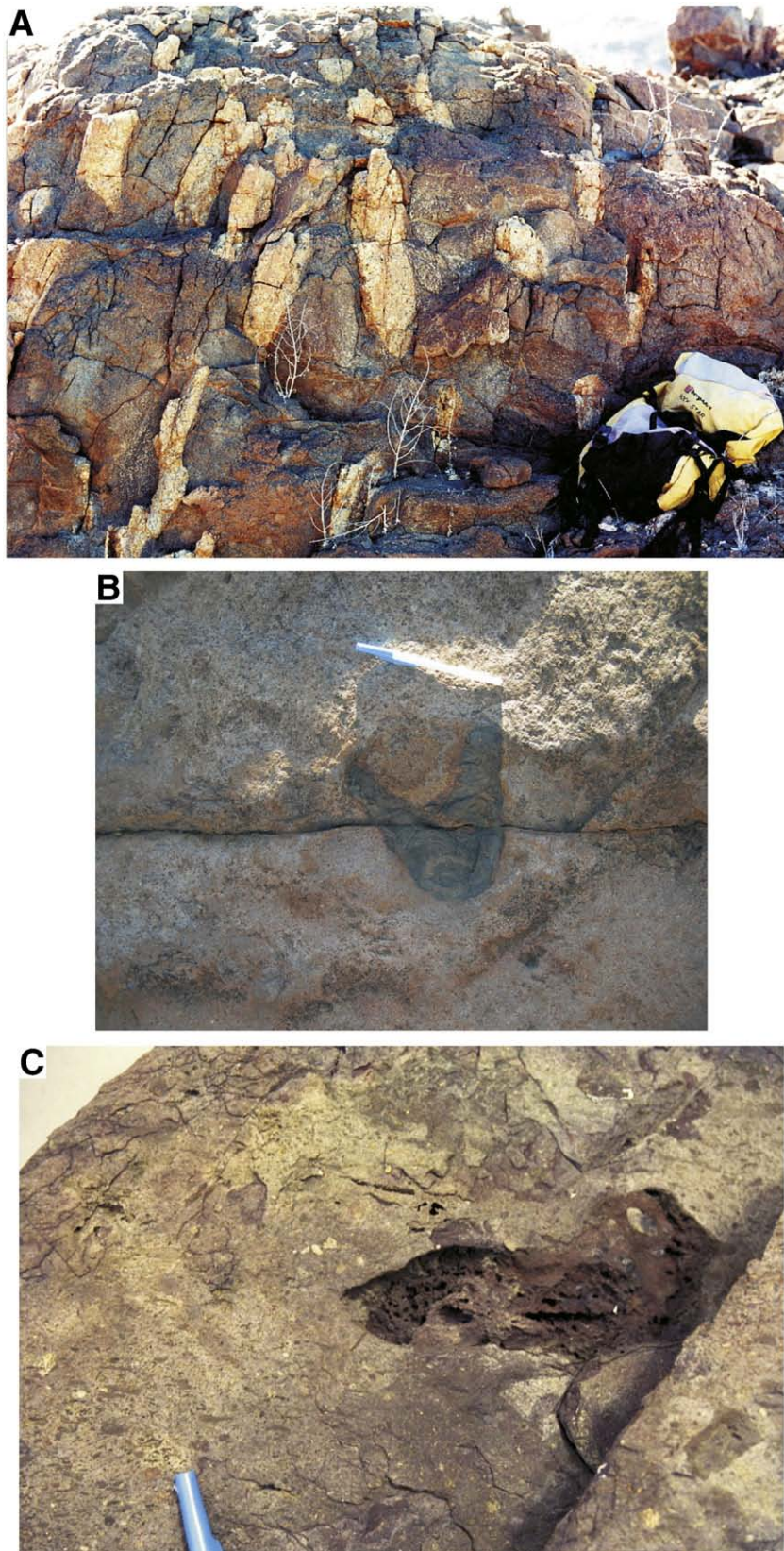


Fig. 3. Textural features illustrating the synchronicity of mafic and silicic magmas in LIPs. A) Mafic and silicic magma interaction producing 'organ-pipes' ($21^{\circ}25.72' S 14^{\circ}16.89' E$), the result of multiple diapirs of granite that have intruded upwards through unsolidified mafic diorite in the easternmost moat of the Messum igneous complex (Paraná–Etendeka LIP; see also Ewart et al., 2002). B) Outsized, ductile deformed and folded juvenile mafic spatter clast within the lava-like Jozini rhyolite (Karoo LIP), Namaacha Falls, Mozambique ($25^{\circ}57.55' S 32^{\circ}02.1' E$). Pen is 15 cm long. C) Outsized, juvenile mafic scoria clast within a densely welded rhyolitic ignimbrite, with the eutaxitic fabric subhorizontal in photo (Whitsunday silicic LIP, Cid Island, northeast Queensland; $20^{\circ}16.341' S 148^{\circ}55.083' E$). Pen lid width is 0.8 cm.

deposits (Bryan et al., 1997), and substantial volumes may actually reside as tephra deposits in ocean basins (e.g., Straub and Schmincke, 1998; Pattan et al., 2002; Ukstins Peate et al., 2005).

A large proportion of the erupted volume may reside in co-ignimbrite ash deposits deposited >1000 km downwind (Sparks and Walker, 1977; Moore, 1991; Self, 1992; Koyaguchi and Tokuno, 1993). Co-ignimbrite ash plumes are generated where the pyroclastic suspension currents lift off at their run-out distance (Freundt, 1999), which may be ≥ 100 km from source, in the largest LIP silicic eruptions. Modelling has predicted that a substantial fraction (30–80%) of the erupted mass is entrained in to co-ignimbrite ash plumes that reach stratospheric heights where the erupted material is then distributed widely (Woods and Wohletz, 1991; Bonadonna et al., 1998). This occurs even during eruptions of relatively low magmatic gas content and high discharge (Freundt, 1999), which may be more characteristic of silicic eruptions in flood basalt provinces. Recent insight into this issue, and the potential extent and increased magnitude of silicic eruptions from LIPs comes from the correlation of deep sea ashes with onshore ignimbrites from the Afro-Arabian LIP (Ukstins Peate et al., 2003, 2008). Conversely, approximately 200 very widely dispersed basaltic to rhyolitic ash layers are preserved in basins adjacent to the North Atlantic LIP (Larsen et al., 2003), but source regions and total erupted volumes remain very poorly constrained.

Deposit dense-rock-equivalent volumes from known large-volume LIP eruptions are listed in Tables 2 and 3. These should be considered as minima. Although studies of some recent >M8 caldera-forming explosive eruptions have indicated that deposit volumes reside in approximately equal proportions as intracaldera (I), outflow (O) and co-ignimbrite ash (A) deposits (Rose and Chesner, 1987; Wilson, 2001), we have not adjusted deposit volumes (applying the assumption that total volume = I + O + A) as suggested by Mason et al. (2004). This is because for the silicic eruptions listed in Table 3: 1) calderas and any potential ignimbrite fill have rarely been identified in LIPs; 2) it remains unclear if these LIP eruptions did lead to true caldera collapse (and what the relative timing of collapse was) and eruptions may have instead produced large regional down-sagging (e.g., Ewart et al., 2002; Mahoney et al., 2008); and 3) while recent efforts have identified distal co-ignimbrite ash deposits for some Afro-Arabian silicic eruptions (Ukstins Peate et al., 2003, 2008) allowing an upward revision of eruptive volumes on the basis of O + A (Table 3), distal co-ignimbrite ash deposits have yet to be positively identified for the Paraná–Etendeka silicic eruptive units. Silicic ash horizons present in some drill cores recovered from the South Atlantic have been dated to an approximate age consistent with Paraná–Etendeka eruptions (Barker et al., 1988). These offer hope that distal ash deposits do exist but substantiation requires further detailed analysis and geochemical comparison (Mawby, 2008). It therefore should be noted that deposit volumes listed in Table 3 for the Paraná–Etendeka silicic eruptive units equate to approximately two-thirds of the total erupted volume (O + I) if co-ignimbrite ash deposits exist.

3. LIP eruptions

LIPs are dominantly basaltic igneous events and the primary volcanic building blocks are extensive (10^3 – 10^5 km²), sheet-like lava flow fields (Fig. 6; e.g., Self et al., 1997; Jerram, 2002; White et al., 2009). However, in continental LIPs (flood basalt provinces and volcanic rifted margins), mafic volcanoclastic deposits (Ross et al., 2005; Ukstins Peate and Bryan, 2008), sill and dyke intrusions (Jerram, 2002; Elliot and Fleming, 2008) and silicic ignimbrites (Bryan et al., 2002; Bryan, 2007) are also, areally and volumetrically significant and important architectural components (White et al., 2009). The largest flood basalts and rhyolites of LIP events have remarkably similar volumes for individual eruptions (Tables 2 and 3).

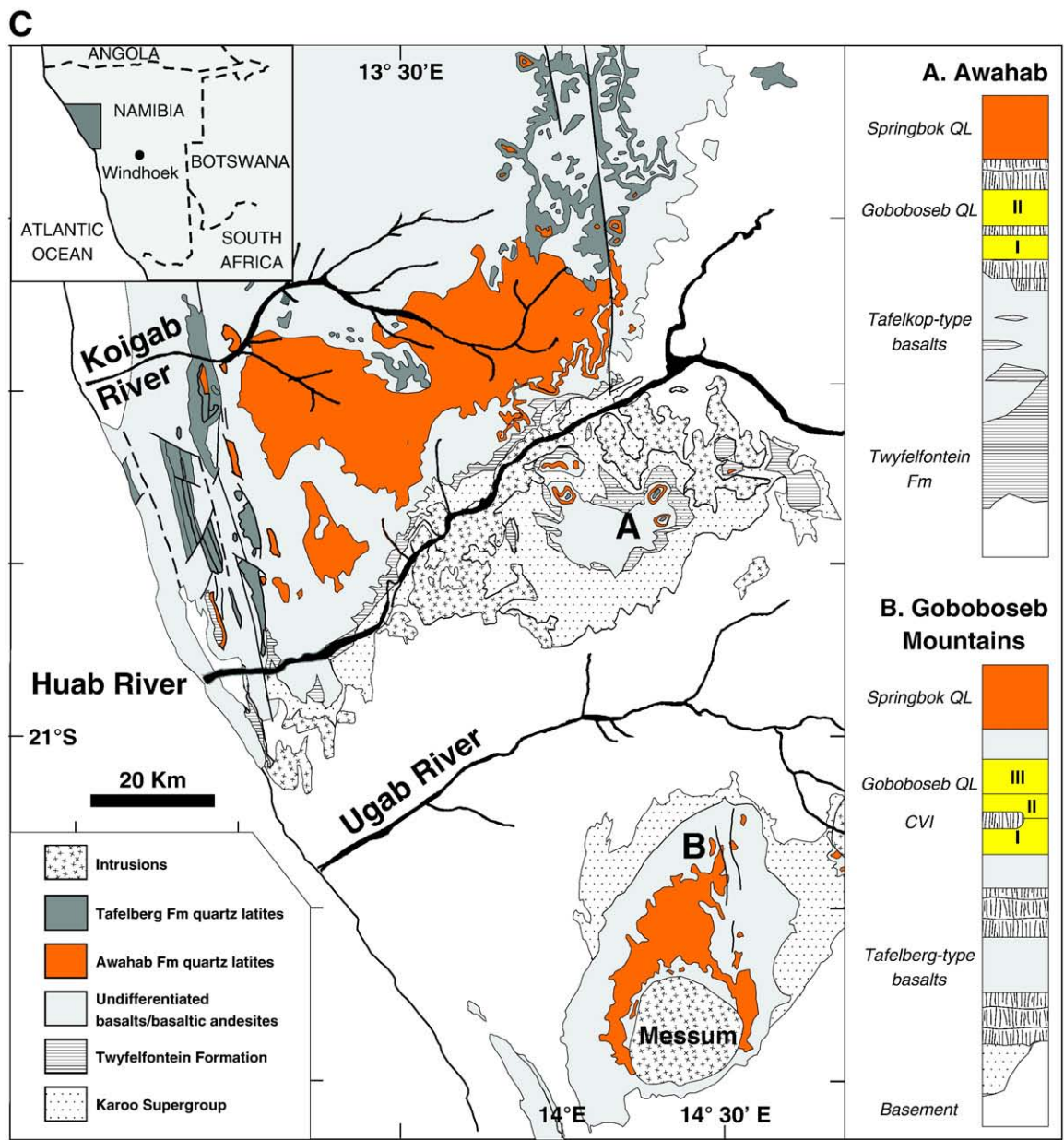
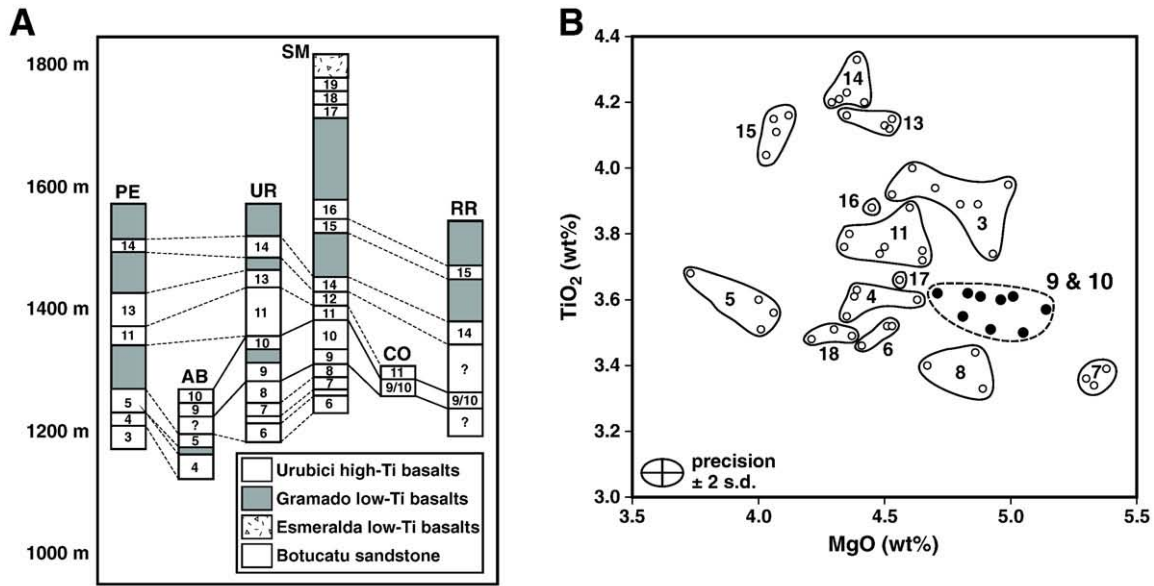
3.1. Flood basalt eruptions in LIPs

The basaltic lava flow fields in LIPs in many cases are so extensive, and the provinces so widespread and fragmented or eroded, that it has taken many years of study to determine what the products of a “typical” flood basalt eruption comprise (White et al., 2009). Most insight into the products of flood basalt eruptions has come from studies on the Columbia River Basalt province (CRB) of northwest USA (see summaries in Tolan et al., 1989; Reidel et al., 1989; Self et al., 1997; Hooper, 1997).

Dominantly pahoehoe lava flow fields form the flood basalt lavas in LIPs. Each flow field is interpreted to be the product of one, but potentially sustained (Self et al., 1997), eruptive event producing several major lava flows that in turn consist of multiple sheet-like flow lobes. The major sheet lobes contain the majority of the lava volume, and in the CRB are commonly 20 to 30 m thick, and several kilometres wide. In the Karoo and Etendeka flood basalt provinces, however, studied sections generally reveal only a few lava flows >20 m thick, suggesting that the majority of the flood lava volume is not always expressed in thick lava flow units. Nevertheless, the flood basalts from these provinces show features consistent with *in situ* flow thickening by endogenous growth and inflation (Self et al., 1997; Bondre et al., 2004; White et al., 2009). These extensive lobes, with aspect ratios (length/thickness) ranging from ~50 to 500, are the basic building-blocks of continental flood basalt provinces and give the provinces their “layer-cake”, or step-like, appearance (Fig. 6A; Jerram and Widdowson, 2005; White et al., 2009). Sheet lobes show a relatively simple internal structure of crust and lava core facies (Fig. 6B, C) that are ubiquitous in the lavas regardless of thickness, and persist over the extent of the entire flow field (10^2 – 10^3 km²; Self et al., 1997; 2008). Parts of some continental flood basalt provinces, e.g., Deccan, are formed of flow-fields dominated by thinner, smaller lava units stacked up to form compound lavas (Walker, 1972; Bondre et al., 2004). Complexities can occur where lava enters lakes or oceans producing pillowed, hyaloclastite and pyroclastic facies (e.g., Waters, 1960; Larsen et al., 2006).

Volcanological studies in the CRB province on the eruptive characteristics of flood basalt eruptions have shown that: 1) at least parts of flood basalt eruptions were Hawaiian-like in nature at the vent (Reidel and Tolan, 1992); 2) the flow fields most likely originated from prolonged eruptions lasting years to decades (Self et al., 1996, 1997, 1998; Thordarson and Self, 1996, 1998), with the larger flow fields fed by very long fissures (e.g., Swanson et al., 1975); 3) the length of flow fields has been supply-limited rather than landscape- or cooling-limited (Stephenson et al., 1998; Keszthelyi and Self, 1998; Keszthelyi et al., 2004; Self et al., 2008), with several reaching the sea >400 km from vent; 4) at any one time, eruptive activity was more likely confined to distinct fissure segments on the vent system (Thordarson and Self, 1998), resulting in incremental flow advancement and flow field growth; and 5) postulated eruption rates of ~ 4000 m³ s⁻¹ (Self et al., 1998) are similar to the maximum sustained eruption rates of the largest historic eruptions (e.g., Laki, Thordarson and Self, 1993). Given the inferred duration and sporadic and restricted activity along the vent fissure system of flood basalt eruptions, defining what the product of one eruption is remains a difficult task in flood basalt studies.

Flood basalt lavas vary from being aphyric or sparsely phyrlic ($\leq 5\%$) to strongly porphyritic (up to 40%) with plagioclase and clinopyroxene usually dominating the phenocryst assemblage. Generally, geochemical data define two compositionally distinct groups of mafic lavas that can be clearly differentiated in terms of immobile high field strength elements (Zr, Ti, Y and Nb) and have been termed low- and high-Ti (>2 wt.% TiO₂) basalts (e.g., Duncan et al., 1984; Peate et al., 1992; Melluso et al., 1995; Ewart et al., 2004a). High-Ti basalts are often mildly alkaline whereas the low-Ti basalts are tholeiitic in composition. The presence of abundant plagioclase in the flood basalts has generally been interpreted to reflect crystallisation at



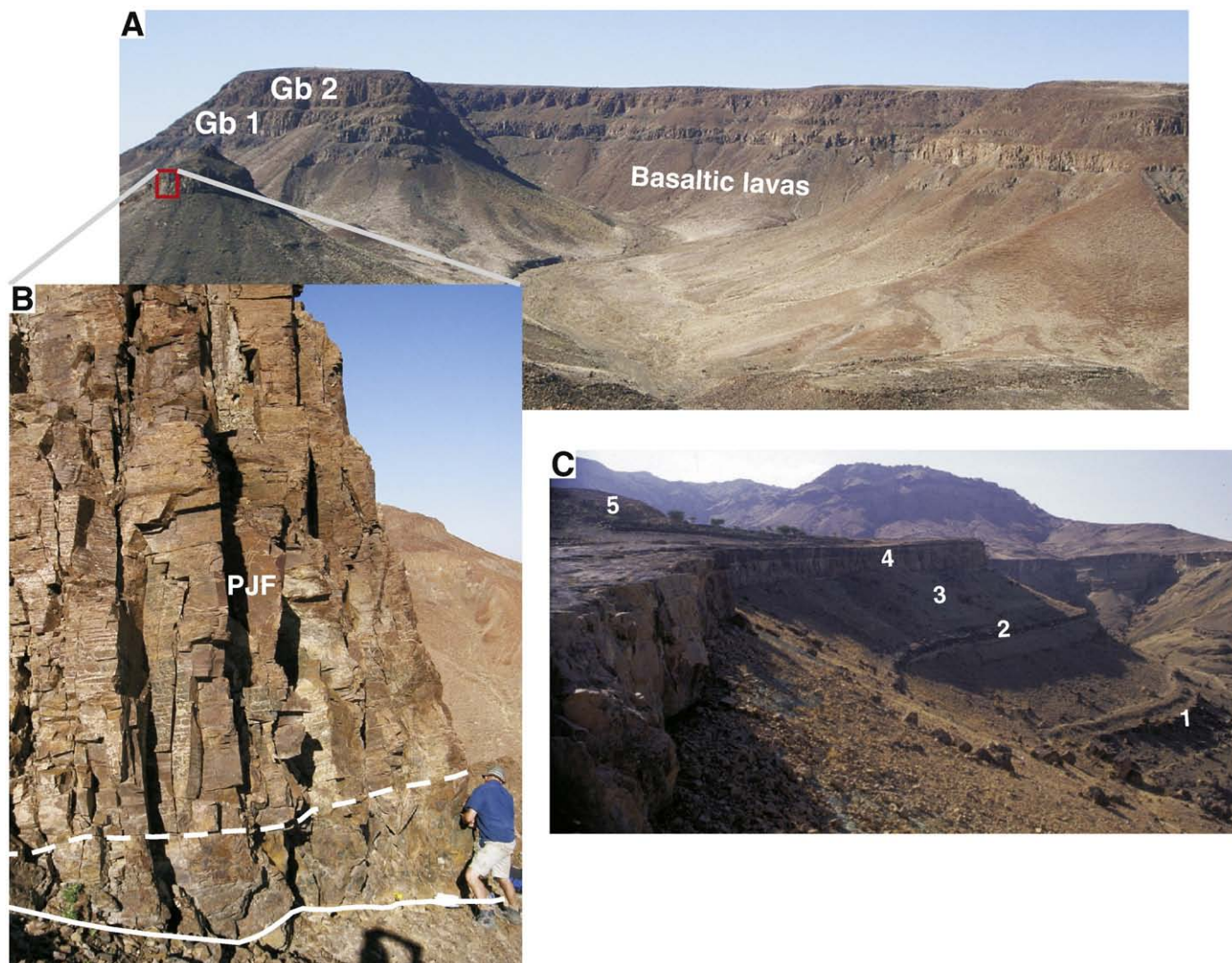


Fig. 5. Examples of large-volume silicic eruptive units from LIPs. A) View northeast towards Tafelkop in the Etendeka ($21^{\circ}07.13'S$ $14^{\circ}17.3'E$) that is capped by two ~ 30 m sheet-like quartz latite rheoignimbrite units (Goboboseb I, Gb 1; Goboboseb II, Gb 2). B) Closeup of base of Goboboseb I in contact with brecciated basaltic lava at base of photo illustrating a typical 'valley-fill' geometry. A basal, discontinuous topography-filling, massive quartz latite facies is overlain by an intensely platy jointed facies (PJF) that is more sheet-like in geometry (boundary between depositional facies marked by dashed line). Location of section shown in A). C) Afro-Arabian main silicic sequence of pyroclastic flow and fall deposits from Bayt Baws, located near Sana'a, Yemen ($15^{\circ}16.5'N$ $44^{\circ}11.3'E$). Main eruptive units, from base to top are: 1) Jabal Kura'a Ignimbrite; 2) Escarpment Ignimbrite; 3) Green Tuff; 4) SAM Ignimbrite; 5) caldera-collapse breccia Iftar Alkalb; conglomerate separates the Escarpment Ignimbrite and Green Tuff (Ukstins Peate et al., 2005). The ignimbrites exhibit distinct tabular morphology, which is recognizable across 100s of km around the Sana'a basin and towards the western escarpment. Total thickness of section is 115 m.

crustal pressures (Cox, 1980), whereas the locally phenocrystic character of some high-Ti lavas has been attributed to the accumulation of mafic phenocryst phases (Hooper, 1997; Ewart et al., 2004a). The aphyric lavas reflect removal of crystals by fractional crystallisation, which is supported by lower MgO and higher SiO₂ contents (Hooper, 1997; Ewart et al., 1998a; 2004a).

3.2. Silicic eruptions in LIPs

Most Quaternary examples of the products of large-volume silicic eruptions (>10 to $1000s$ km³) are related to Plinian and pyroclastic

flow-forming explosive eruptions where a regular eruptive sequence of widespread pumice and ash fallout accompanied, and was followed by, the emplacement of voluminous ignimbrites leading to caldera collapse, and later, post-collapse extrusion of relatively small-volume rhyolitic lava flows and domes (e.g., Valles, Taupo, Yellowstone, Long Valley calderas; Walker, 1981; Miller and Wark, 2008; Wilson, 2008; cf. Branney et al., 2008). Plinian fall deposits, which have accompanied many of the recent examples of silicic super-eruptions (Wilson, 2008) are extremely rare in LIPs. This is despite rapid accumulation rates of the volcanic piles and limited evidence for intra-LIP erosion that might remove such deposits. Some examples are known of distal ash

Fig. 4. Potential examples of contemporaneous eruptions in LIPs. A) Local correlation of Urubici lava flows in the São Joaquim area (Peate et al., 1999) with local topographic relief controlling the emplacement of early lava flow units (3–8). PE, Perico; AB, Aguas Brancas; UR, Urubici; SM, Morro do Igreja; CO, Corvo Branco; RR, Rio Rufino sections of Peate et al. (1999). B) Compositional plot of MgO–TiO₂ showing the similarity of basaltic lava units 9 and 10 and their difference to other Urubici high-Ti lava flow units. The basaltic lava interbedded with the Urubici units 9 and 10 in the UR profile is sample DUP-38 (from Peate and Hawkesworth, 1996) that is an evolved Gramado-type basalt with 3.3 wt.% MgO and 1.68 wt.% TiO₂. C) Simplified map of southern Etendeka showing the distribution of the Etendeka flood volcanic succession and schematic stratigraphic sections for the Awahab and Goboboseb Mountain area (modified from Jerram et al., 1999) where two compositionally different mafic lava units separate units 1 and 2 of the Goboboseb quartz latite. In the Goboboseb Mountains, the Copper Valley icelandite (CVI, Ewart et al., 1998a) lies stratigraphically between Goboboseb units 1 and 2, whereas chemically different, low-Ti-type basalts separate these quartz latite units in the Awahab area. QL, quartz latite.

Table 1
Prospectivity assessment of Late Paleozoic to Neogene continental LIPs for the future discovery and definition of large-magnitude (>M8 or 10^{15} kg magma) eruptive units.

LIP (age of activity) (Ma)	>M8 basaltic	>M8 silicic	Comments
Columbia River (17–6)	High	High	Flat-lying to generally gently folded lava units; stratigraphy well-constrained and mapped flood basalt succession supported by detailed geochemical database. Silicic eruptive units of comparative age residing in adjoining Snake River Plain province
Afro-Arabian (31–14)	Moderate	High	Large-magnitude silicic eruptive units previously described; flat-lying stratigraphy offers promise for future recognition of products of large-magnitude flood basalt eruptions.
Sierra Madre Occidental (38–17)	None	High	Flat-lying stratigraphy and limited erosion, but locally deeply incised providing some cross-sectional exposure. Although largely unexplored (~10% of province has been mapped in any detail), access is improving. High prospectivity for determining products of large-magnitude silicic eruptions given existence of many large-magnitude eruptive units of similar age along strike to north in western USA. Associated basaltic products are small-volume and unlikely to define large-magnitude eruptions.
North Atlantic (62–53)	Moderate	Low	Recognition of large-magnitude eruptions hampered by tectonic fragmentation, large eruptive volumes stored in offshore sequences, and deeper level of exhumation of the British Tertiary Igneous Province. Excellent exposure and field correlations of lava packages exist for West Greenland but have low total exposed volume; greater potential exists for thicker and more extensive East Greenland successions. Silicic magmatism almost absent from Greenland but is more abundant in the eroded British sequences.
Deccan (67–60)	High	Low	Flat-lying to gently warped lava pile; improving constraints on lava flow stratigraphy, ages, chemistry and palaeomagnetism offer reasonable potential for identifying large-magnitude flood basalt eruptions as much of province is intact, but mostly poorly exposed. More distal northern and western parts not yet correlated with main Deccan province. Associated silicic volcanism is small-volume, and unlikely to define large-magnitude eruptions.
Madagascar (90–84)	Moderate-Low	Low	Relatively narrow, eroded and tilted, rifted margin successions with widespread erosion and weathering; geochemical database improving. Some potential for flood basalt \pm rhyolite correlation between Volcan de l'Androy and Morondava Basin successions. Rhyolite and dacites recently correlated with the conjugate margin of SW India.
High Arctic (130–80)	Low	Low	Giant continental dyke swarm, sill and mafic-ultramafic intrusive province where volcanic portion has been largely removed by erosion, is partly submerged beneath Arctic Ocean and has undergone tectonic fragmentation.
Whitsunday (132–95)	None	Moderate-Low	Tilted, partly submerged sections along rifted margin hinder areal extent definition to eruptive units. Associated basalts are small-volume and unlikely to define large-magnitude eruptions.
SW Australia (Bunbury)-Comei (~135–100)	Low	Low	Volcanics predominantly preserved on submerged basaltic plateaux off SW Australia; onshore portion (Bunbury basalt) is limited; The volcanic portion of the Comei LIP remnant largely removed by erosion exposing subvolcanic intrusions.
Paraná–Etendeka (138–125)	High	High	Generally flat-lying stratigraphy, well-constrained silicic eruptive stratigraphy for Etendeka and limited erosion in Paraná; extensive geochemical database. Large areas of southern Angola on Etendeka side, and massive unexposed volumes on Paraná side mean a high potential for future identification of large-magnitude eruptions (both mafic and silicic), but generally very limited exposure in Paraná will hamper progress in this regard. Submerged volcanic rifted margin and marginal plateaux, with only limited drill hole and dredge sampling undertaken.
NW Australia (165–155)	Low	Low	Extensive post-LIP erosion and limited exposure due to snow/ice sheet cover and faulting hampers areal extent definition. Sills are dominant expression of magmatism, and a number of large-magnitude intrusions already identified. Restricted exposure of silicic volcanic rocks occurs in the basal Hanson Formation, which contains a significant resedimented component, and a likely record of distal eruptions indicates a low prospectivity for large-magnitude silicic eruptions.
Ferrar (185–175)	Moderate-Low	Low	Generally flat-lying stratigraphy in Patagonia, but sequences are deformed and tilted in the Andean Cordillera of Argentina. Little detailed mapping, variable exposure and faulting have hindered stratigraphic correlations. Concealment, faulting and physical weathering affect exposures in the Antarctic Peninsula. Associated basalts are small-volume and unlikely to define large-magnitude eruptions.
Chon Aike (188–153)	Low	High	Tilted stratigraphy in Lebombo section precluding areal extent definition to silicic eruptive units. Lesotho Formation basalts offer most prospectivity but is complicated by the likely eruption from a widespread network of fissures precluding the formation of a single large, long run-out flow. Potential exists for defining large-magnitude intrusions or coupled lava-feeder intrusive units.
Karoo (190–178)	Moderate	Low	Basaltic lavas predominantly occurring as tectonically fragmented remnants within rift basins of North America and northwest Africa, with a substantial volcanic volume removed by erosion. Most onshore preservation is as continental dyke swarms, sills and mafic-ultramafic intrusions; a higher prospectivity exists for defining large-magnitude intrusions or coupled lava-feeder intrusive units.
Central Atlantic (205–191)	Low	Low	Large areas of province are buried/unexposed with extensive subcrops of basalt occurring beneath the West Siberian Basin. Limited detailed mapping in many areas due to exposure and seasonality of outcrop access. Wide extent and large volumes of mafic volcanoclastic deposits and intrusions offer possibility for large-magnitude basaltic hydromagmatic eruptions and sills, respectively. Improving geochemical and geochronological database. Silicic igneous rocks are volumetrically minor, and unlikely to yield large-magnitude eruptive units.
Siberian Traps (254–248)	Moderate	Low	Tilted and faulted sections, significant erosional dissection, and lack of detailed lava litho- and chemostratigraphy. Associated silicic volcanism is small-volume, although the Wangpo bed offers potential. Mafic volcanoclastic deposits may offer more potential than associated flood basalt lavas.
Emeishan (261–251)	Moderate	Low	Majority of the igneous rocks buried by a thick succession of post-Permian strata and folded and faulted by Cenozoic deformation. Province extent and volume estimates largely based on geophysical data.
Tarim (292--270)	Low	Low	

deposits preserved in adjacent sedimentary or marine basins that correlate to the terrestrial flood volcanism (Heister et al., 2001; Larsen et al., 2003) and in some cases are co-ignimbrite in origin (Ukstins Peate et al., 2003, 2005).

Rhyolite lavas tend to be small volume (<100 km³) and uncommon in the continental flood basalt provinces, but although more common in the silicic LIPs (Bryan et al., 2002; Bryan, 2007), are

similarly small in volume <100 km³. Volumetrically significant accumulations and individual lava units (up to ~2,000 km³) are known from a few Proterozoic provinces (Rooiberg Felsite/Bushveld igneous complex/LIP, South Africa, Twist and French, 1983; North Shore Volcanic Group/Keeweenaw Rift, Minnesota, Green and Fitz, 1993), and the most detailed studies have recently been published on lavas from the Gawler Range Volcanics, South Australia (Allen and

Table 2

Catalogue of the largest known mafic eruptive units from LIPs ($\geq 1300 \text{ km}^3$) ordered in terms of eruptive volume. The Mesozoic to Cenozoic LIPs are the best studied and preserved and the catalogue is biased to these more modern examples. For the basaltic eruptions, the Columbia River flood basalt province may contain more than 300 individual basalt lava flows that have an average volume of 500–600 km^3 (Tolan et al., 1989). Eruptive volumes are dense rock equivalent. Eruption magnitude is based on Pyle (1995, 2000) using a magma density of 2700 kg m^{-3} . Note that the eruptive volume for the Mahabaleshwar–Rajahmundry Traps eruptive unit is an upper end of a plausible range of eruptive volumes for this pahoehoe lava flow field that reached across the Indian subcontinent (see Self et al., 2008).

Eruptive Unit	LIP	Eruptive Age (Ma)	Minimum Eruptive Volume (km^3)	Lithology and Thickness (m)	Magnitude	Composition (wt.% SiO_2)	References
Mahabaleshwar–Rajahmundry Traps (Upper)	Deccan	64.8	9300	Basalt lava (20–50)	9.40	High-Ti tholeiitic Basalt (48.1)	Self et al. (2008)
McCoy Canyon flow (Sentinel Bluffs Member, Grande Ronde N_2)	Columbia River	15.6	4278	Basalt lava (10–60)	9.06	Tholeiitic Basalt (53.6)	Reidel (2005); Landon and Long (1989)
Umtanum flow (Grande Ronde N_2) ¹	Columbia River	~15.6	~2750	Basalt lava (~50)	8.87	Tholeiitic Basalt (54.7)	Reidel et al. (1989)
Sand Hollow flow (Frenchmans Springs member, Wanapum Basalt)	Columbia River	15.3	2660	Basalt lava (~40)	8.86	Tholeiitic Basalt (51.8)	Beeson et al. (1985) Tolan et al. (1989)
Pruitt Draw flow (Teepee Butte Member, Grande Ronde R_1)	Columbia River	16.5	2350	Basalt Lava (30–100)	8.80	Tholeiitic Basalt (53.0)	Reidel and Tolan (1992); Reidel (1983)
Museum flow (Sentinel Bluffs Member, Grande Ronde N_2)	Columbia River	15.6	2349	Basalt Lava (10–80)	8.80	Tholeiitic Basalt (54.2)	Reidel (2005); Landon and Long (1989)
Rosalia flow (Priest Rapids Member, Wanapum Basalt)	Columbia River	14.5	1900	Basalt lava (~50)	8.70	Tholeiitic Basalt (50.5)	Tolan et al. (1989)
Joseph Creek flow (Teepee Butte Member, Grande Ronde R_1)	Columbia River	16.5	1850	Basalt Lava (20–90)	8.70	Tholeiitic Basalt (52.3)	Reidel and Tolan (1992)
Ginkgo Basalt (Frenchmans Springs member)	Columbia River	15.3	1600	Basalt lava (30–>150)	8.64	Tholeiitic Basalt (51.5)	Tolan et al. (1989); Reidel et al. (1994); Beeson et al. (1985)
Rosa Member (Wanapum Basalt)	Columbia River	14.5	1300	Basalt lava (3–50)	8.55	Tholeiitic Basalt (50.2)	Tolan et al. (1989); Self et al. (1997)
Stember Creek flow (Sentinel Bluffs Member, Grande Ronde N_2)	Columbia River	15.6	1192	Basalt lava (5–50)	8.51	Tholeiitic Basalt (53.5)	Reidel (2005); Landon and Long (1989)

1. Reidel et al. (1989) recognised the Umtanum unit comprised 2 lava flow units with a cumulative volume of $>5500 \text{ km}^3$, but an average of 2750 km^3 for each lava flow.

McPhie, 2002; Allen et al., 2003; 2008). In addition to these eruptive products, similarly extensive and voluminous high-level, lava-like rhyolitic sills have been described and interpreted from ancient and partly exhumed LIPs (Trendall, 1995).

Large-volume rhyolitic ignimbrites in LIPs vary in deposit facies characteristics from extremely lava-like, but showing ignimbrite depositional geometries (Fig. 5; e.g., Parana–Etendeka quartz latites, Milner et al., 1992; Mawby et al., 2006; Mawby, 2008) to “Snake River Plain”-type (Branney et al., 2008) or high-grade ignimbrites with some preservation of pyroclastic textures (e.g., Karoo rhyolites; Bristow, 1976; Cleverly, 1977; 1979) to more commonplace, low- to high-grade welded ignimbrites containing abundant pumice lapilli and fiamme, rock fragments and well-preserved vitriclastic textures (e.g., North Atlantic Igneous Province, Bell and Emeleus, 1988; Afro-Arabian province, Ukstins Peate et al., 2005; Silicic LIPs, Bryan et al., 2002; Bryan, 2007). This textural variation is most likely related to differing eruptive and emplacement temperatures and volatile contents of the magmas (Branney & Kokelaar, 1992; Kirstein et al., 2001; Ukstins Peate et al., 2005; Branney et al., 2008). A common characteristic of the major silicic eruptive units in LIPs is that they generally form relatively massive, monotonous sheet-like ignimbrite units (Fig. 5A, C), lacking evidence for internal bedding or time breaks (cf. Wilson, 2008). The silicic eruptive units do show lateral thickness variations due to ponding relationships in topographic (Fig. 5B) or structural depressions or with proximity to vent (Ewart et al., 1998b; 2004b; Ukstins Peate et al., 2005).

Additional features shared by the large-volume rhyolites in LIPs are their: 1) silica-rich bulk chemical composition (~68–75 wt.% SiO_2); and 2) general lateral and chemical homogeneity, yet they are chemically distinct from other interbedded silicic eruptive units (e.g., Milner et al., 1995; Trendall, 1995; Marsh et al., 2001; Miller and Harris, 2007). Significantly, phenocryst assemblage is not diagnostic of eruptive volume, being highly variable and ranging from typically crystal-poor (<10% modal phenocrysts) and anhydrous assemblages in the continental flood basalt provinces to ignimbrites with high phenocryst contents (up to 50%) and hydrous mineral assemblages in

the silicic LIPs (Bryan, 2007), as well as those from extensional continental margin settings (Mason et al., 2004). The latter ignimbrite examples are equivalent to the better-known ‘monotonous intermediate’ ignimbrites (e.g., Hildreth, 1981; Maughan et al., 2002) such as the Fish Canyon Tuff (Lipman et al., 1970; Bachmann et al., 2002). This variation in phenocryst assemblage partly reflects significant differences in magma temperature with the crystal-poor rhyolites from the continental flood basalt provinces being higher-temperature ($>1000 \text{ }^\circ\text{C}$) eruptives (e.g., Milner et al., 1992; Streck and Gruner, 2008; cf. Bachmann and Bergantz, 2009).

4. Magnitude of LIP eruptions

Constraints on flood basalt eruption magnitudes come mostly from the well-studied CRB province, which is the product of many, dominantly pahoehoe flow fields varying in size from 1 to $>2000 \text{ km}^3$ in volume (Tolan et al., 1989). The recent study of Reidel (2005) of proposed chemically correlated flow types such as the McCoy Canyon or Cohasset (Table 2) of the Grande Ronde Basalt Formation, indicates much larger volume flows may have been emplaced during the interval when $>60\%$ of the volume of the CRB province was erupted (Tolan et al., 1989; Camp et al., 2003). Also, studies on the Ambenali and Mahabaleshwar Formations of the Deccan indicate single formations have volumes similar to the entire CRB Group ($\sim 0.234 \text{ Mkm}^3$, Camp et al., 2003), with volumes of individual flow fields ranging from ~ 2000 to $>8000 \text{ km}^3$ (Self et al., 2006; 2008). This general upper magnitude for flood basalt lavas is similar to the dimensions of associated sills in flood basalt provinces, such as the enormous Penneplain Sill in the Dry Valleys, Antarctica, ($19,000 \text{ km}^2$; Gunn and Warren, 1962) with an estimated volume of 4750 km^3 , the Dufek-Forrestal intrusions ($10,200$ – $11,880 \text{ km}^3$; Ferris et al., 1998), and the 1500 to 5000 km^3 Palisades Sill of the Central Atlantic Magmatic Province (Husch, 1990; Gorrington and Naslund, 1995).

The magnitude of silicic eruptions in LIP events, by contrast, has received little attention with a presumption that the flood basalt

Table 3
 Compilation of the largest known silicic eruptive units from LIPs (>1500 km³ dense rock equivalent) ordered in terms of eruptive volume/magnitude. Eruption magnitudes (Pyle, 1995; 2000) are based on magma densities of 2500 kg m⁻³ for the Paran -Etendeka quartz latites, and 2400 kg m⁻³ for the Afro-Arabian and Gawler Range rhyolites. Areal extents of correlated eruptive units from the Paran -Etendeka province are shown in Fig. 7. For comparison, the 74 ka Toba eruption from Indonesia evacuated the equivalent of 2700 km³ of magma, and the Fish Canyon Tuff at 4500 km³ dense rock equivalent volume, is the most commonly cited example of the largest known ignimbrite eruption (see references in Mason et al., 2004). The ~132 Ma eruptions of the PAV-B/Springbok and Guarapuava-Tamarana/Sarusas quartz latites in the Paran -Etendeka Province evacuated ~1.7 and ~2.1 times more magma than the Fish Canyon Tuff, respectively.

Eruptive Unit	LIP	Eruptive Age (Ma)	Minimum Eruptive Volume (volume basis) DRE ¹ (km ³)	Lithology and Thickness (m)	Magnitude	Composition SiO ₂ (wt.%)	References
Guarapuava (P ₂ O ₅ <0.44 wt.%) - Tamarana/Sarusas ²	Paran�-Etendeka	132	8587 (O)	Rheoignimbrite (50–120)	9.33	High-Ti Quartz Latite (67.2/64.3)	Marsh et al. (2001); Ewart et al. (2004b); Peate et al. (1992); Nardy et al. (2008)
Santa Maria/Fria	Paran�-Etendeka	~132	7808 (O)	Rheoignimbrite (100–200)	9.29	Low-Ti Quartz Latite (70.5)	Marsh et al. (2001); Ewart et al. (2004b); Garland (1994); Nardy et al. (2008)
Guarapuava (P ₂ O ₅ >0.44 wt.%) / Ventura ²	Paran�-Etendeka	~132	7571 (O)	Rheoignimbrite (45–>70)	9.28	High-Ti Quartz Latite (65.5)	Marsh et al. (2001); Ewart et al. (2004b); Nardy et al. (2008)
PAV B-Caxias do Sul /Springbok ³	Paran�-Etendeka	132	6866 (O)	Rheoignimbrite (250)	9.23	Low-Ti Quartz Latite (68.2)	Milner et al. (1995); Marsh et al. (2001); Renne et al. (1996); Whittingham (1991)
PAV F-Caxias do Sul/Grootberg	Paran�-Etendeka	~132	5651 (O)	Rheoignimbrite (100)	9.15	Low-Ti Quartz Latite (68.2)	Milner et al. (1995); Marsh et al. (2001); Nardy et al. (2008)
PAV A-Jacui/Goboboseb II ⁴	Paran�-Etendeka	132	4348 (O)	Rheoignimbrite (70)	9.04	Low-Ti Quartz Latite (67.5)	Milner et al. (1995); Marsh et al. (2001); Ewart et al. (1998b); Nardy et al. (2008)
Ourinhos/Khoraseb	Paran�-Etendeka	~132	3929 (O)	Rheoignimbrite (60–140)	8.99	High-Ti Quartz Latite (68.0)	Marsh et al. (2001); Ewart et al. (2004b); Garland (1994)
PAV G-Anita Garibaldi/Beacon	Paran�-Etendeka	132	3452 (O)	Rheoignimbrite (40–140)	8.94	Low-Ti Quartz Latite (66.6)	Milner et al. (1995); Marsh et al. (2001)
Iftar Alkalb - Tephra 4 W	Afro-Arabian	29.5	2667 (O + A)	Ignimbrite lag breccia, co-ignimbrite ash (70–>150)	8.81	Rhyodacite (~68)	Ukstins Peate et al. (2005; 2008)
SAM Ignimbrite - Tephra 1W63	Afro-Arabian	29.5	2330 (O + A)	Welded to nonwelded ignimbrite, co-ignimbrite ash, (≤25)	8.75	Rhyolite (72.5)	Ukstins Peate et al. (2003, 2005; 2008)
Moonaree Dacite	Gawler Range	1591	2047 (O)	Dacitic lava (~250)	8.7	Rhyodacite (66.8–69.2)	Allen et al. (2003, 2008)
Palmas BRA-21/Wereldsend	Paran�-Etendeka	132	1875 (O)	Rheoignimbrite (35–480)	8.67	Low-Ti Quartz Latite (69.1)	Milner et al. (1995); Marsh et al. (2001)
Jabal Kura'a Ignimbrite - Tephra 5 W	Afro-Arabian	~29.6	1627 (O + A)	Welded ignimbrite, co-ignimbrite ash (5–9)	8.59	Rhyolite (71.9)	Ukstins Peate et al. (2003, 2005; 2008)
Sana'a Ignimbrite - Tephra 2W63	Afro-Arabian	~29.5	1593 (O + A)	Welded ignimbrite, co-ignimbrite ash (5)	8.58	Rhyolite (74.6)	Ukstins Peate et al. (2005; 2008)

1. Volume estimates are based on preserved outflow volume (O), ash fall volume (A); geochemical correlations between onshore silicic units and Indian Ocean deep-sea tephra layers (Ukstins Peate et al., 2003) have enhanced eruptive volume estimates from the Afro-Arabian LIP. In contrast, no distal ash layers have yet been identified that correlate to the Paran -Etendeka rheoignimbrites, but their eruptive volumes could be 2 to 3 times greater than the listed estimates if distal tuffs are identified. Given the effusive eruptive nature for the Moonaree Dacite, no additional erupted volume is expected to reside as ash fall deposits.

2. The Chape  quartz latite suite of Bellieni et al. (1986) has been subdivided into three by Nardy et al. (2008) with the Tamarana quartz latites distinguished by having intermediate TiO₂ and P₂O₅ contents, which best correlates with the Sarusas quartz latite of the Etendeka (Fig. 8), but as mapped, consists of multiple cooling units based on the work of Ewart et al. (2004b). The high P₂O₅ (>0.44 wt.%) Chape  group quartz latites are interpreted here to correlate with the Ventura quartz latite of the Etendeka province.

3. The volume estimate has been revised slightly upward from Milner et al. (1995) using the reconstruction map of Nardy et al. (2008).

4. Although generally considered as one silicic unit, units 1 and 2 of the Goboboseb quartz latite are locally separated by basalt (Fig. 4C; Milner and Ewart, 1989), and may be the products of two but very closely spaced eruptions. Geochemical comparisons (Milner et al., 1995; this study) indicate the PAV-A quartz latite of the Paran  most closely corresponds to Goboboseb unit 2; field studies in the Etendeka (Milner, 1988; Ewart et al., 1998b) indicate Goboboseb unit 3 is only locally preserved in the Goboboseb Mountains and proximal to Messum.

eruptions were larger in volume and more likely to perturb climate (cf. Cather et al., 2009). The potential scale of silicic eruptive units emplaced during LIP events was first realised by the work of Milner et al. (1992, 1995) in the southern Etendeka continental flood basalt province and through correlations with its rifted counterpart, the Paran  province in South America. This database of extremely large silicic eruptions during LIP events (Table 3) has recently been expanded following detailed studies in the northern Etendeka (Marsh et al., 2001; Ewart et al., 2004b) and Afro-Arabian province (Ukstins Peate et al., 2003, 2005, 2008).

Areal extents of correlated quartz latite units from the Paran -Etendeka LIP are shown in Fig. 7. The areal extents of the quartz latite units indicated by cross-South Atlantic correlations of Milner et al. (1995) and Marsh et al. (2001) are huge (>0.1 Mkm²), ranging up to 0.17 Mkm² and greatly exceeding areas of the largest mapped flood

basalt lavas from the CRB Province (0.01–0.1 Mkm²; Tolan et al., 1989; Self et al., 1997). Lateral extents of the Paran -Etendeka quartz latites are also correspondingly large (up to 650 km; Milner et al., 1995; Marsh et al., 2001) and equivalent to the longest run-out lengths of flood basalt lavas (Tolan et al., 1989). As emphasised in previous correlations (Milner et al., 1995; Marsh et al., 2001), a distinct asymmetry exists in the quartz latite distributions, occupying more area on the South American continent, as well as there being a strong linear distribution to most of the quartz latite units with a preferred NW–SE orientation (Fig. 7). Additionally, a spatial variation exists with the high-Ti quartz latites restricted to the northern area of the Paran -Etendeka province (Bellieni et al., 1986; Peate et al., 1992; Marsh et al., 2001; Ewart et al., 2004b).

Geochemical correlations for the silicic units have been revised and reassessed here since the studies of Milner et al. (1995) and

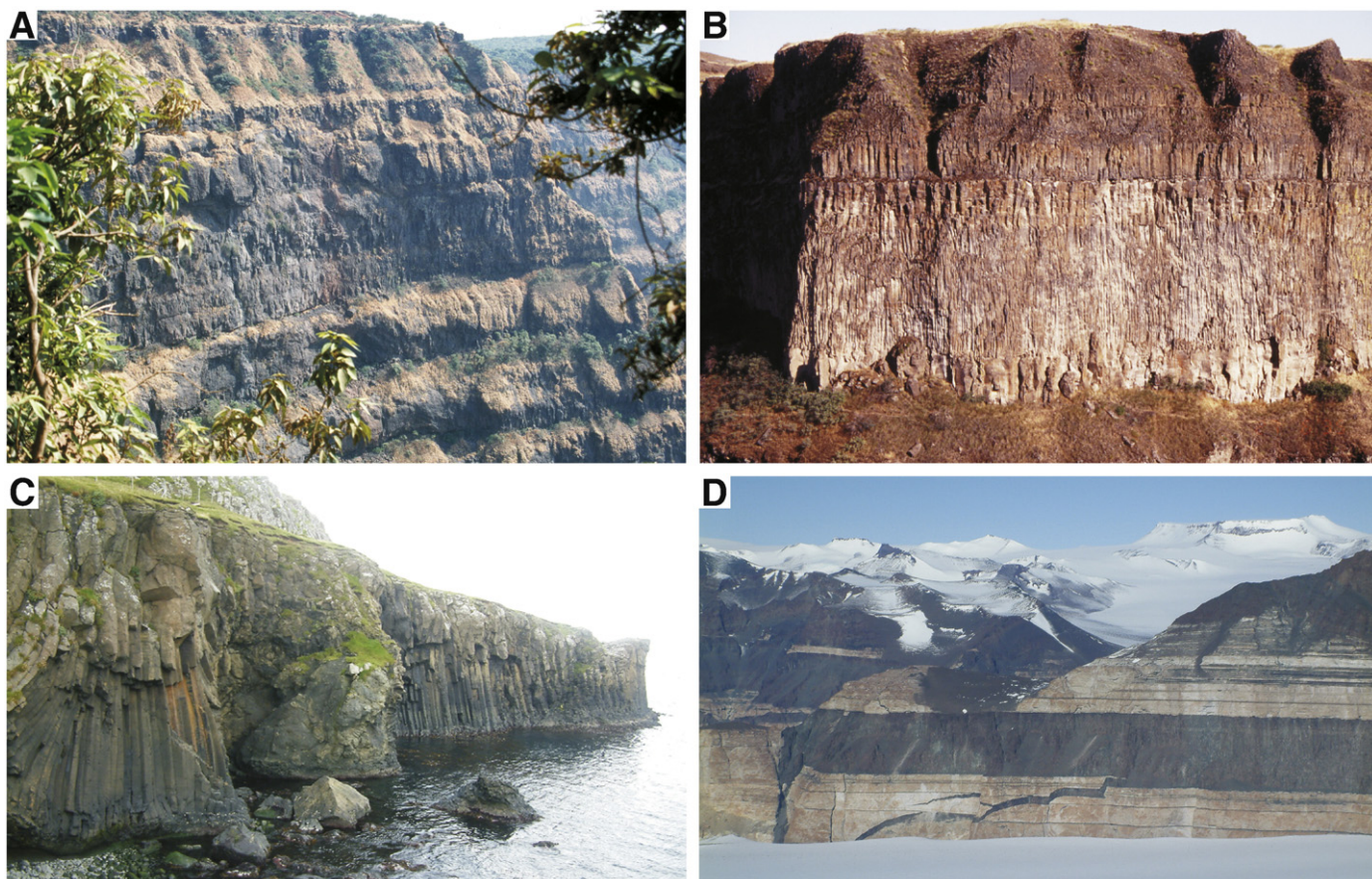


Fig. 6. Examples of large-volume basaltic units from LIPs. A) Deccan lavas from the Wai Sub-Group at Arthur Seat in the Western Ghats near Mahabaleshwar, India ($17^{\circ}58.780' N$ $73^{\circ}38.225' E$), showing several major basalt lava sheet lobes. The main parting in the middle of the photo is the base of a 60 to 70-m-thick sheet lobe. Below this, three thinner (~20 m thick) sheet lobes show sloping, vegetated upper crustal zones and cliff-forming lava cores. The core-upper crust level in the thick sheet lobe is a horizon with overhangs, and the top of the lobe is the lower of two small, prominent cliff lines. Above this is a vegetated slope capped by another cliff-line (near top of photo), which is another flow-field composed of smaller (~100 m long \times 10 m thick) inflated pahoehoe lobes without thick cores. B) Overview of the Sand Hollow flood basalt flow (Table 2) illustrating the internal morphology of a single, large-magnitude ~60 m thick sheet lobe. An upper and lower zone of wider-spaced joints in core of lobe are separated by a more closely spaced central jointed zone. Darker, slightly banded, and gullied part approximates the upper crustal zone of the lobe (top removed by erosion); base is in vegetated slope. Palouse Falls ($46^{\circ}39.730' N$ $118^{\circ}13.554' W$), Columbia River LIP. C) Coastal exposure of basaltic lava flow unit showing well-developed colonnade and entablature jointing, near Trongisvágur, Suðuroy Island, Faroes (North Atlantic LIP). D) Overview of the ~300 m thick Finger Mountain Sill of the Jurassic Ferrar Dolerite, Upper Taylor Glacier, Antarctica ($77^{\circ}44.45' S$ $160^{\circ}42.78' E$), intruded into the Beacon Sandstone Formation; part of the Dry Valleys nested sill complex and plumbing system for the Kirkpatrick flood basalts (Ferrar LIP).

Marsh et al. (2001) utilising new geochemical data, and further chemostratigraphic subdivisions of the Paraná rhyolites by Nardy et al. (2008). In particular, the geochemical correlation of the Guarapuava and Sarusas quartz latites by Marsh et al. (2001) is modified here, as there are consistent compositional differences between the major element data that are most likely outside analytical error. The overall compositional similarity, however, does suggest both were sourced from the same magmatic system. The recent study of Nardy et al. (2008) indicates the Guarapuava, as previously defined, is a composite unit and can be subdivided into two suites distinguished particularly by TiO_2 and P_2O_5 ; the Guarapuava is now restricted to compositions with $TiO_2 > 1.47$ wt.%, and the new 'Tamarana' encompasses compositions with TiO_2 contents between 1.29 and 1.47 wt.% (Nardy et al., 2008). Based on new geochemical comparisons (Fig. 8), it is proposed here the Guarapuava correlates with the Ventura, and the Tamarana with the Sarusas quartz latites from the northern Etendeka (Ewart et al., 2004b). Using stratigraphic controls from the northern Etendeka province (Marsh et al., 2001; Ewart et al., 2004b), these are interpreted to represent the products of different eruptions, but further noting that multiple eruptive (cooling) units suggest the Sarusas quartz latite as mapped by Ewart et al. (2004b), may also comprise the products of more than one eruption.

An important feature of the Paraná–Etendeka LIP is that the likely eruptive source is known for two units – the Goboboseb and

Springbok quartz latites, which have been correlated with the PAV-A and -B rhyolites, respectively, from the Paraná (Milner et al., 1995). This has allowed some perspective to be gained on run-out distances, emplacement directions, and potentially, proximal-distal changes. However, as noted by Milner et al. (1995), geochemical data for the Paraná PAV-A and PAV-B rhyolites, unlike other correlated silicic units, do not correspond precisely with their Etendeka counterparts, and they suggested that at least for the PAV-B unit, it either has been eroded from the top of the Springbok quartz latite in the Etendeka, or that it represents a similar quartz latite but different eruptive unit overlying the Springbok. Ewart et al. (1998b) described vertical and lateral variations in petrography for these quartz latites, and that phenocryst contents decreased with distance for the Springbok PAV-B unit. Significantly, variation between these Etendeka and correlative Paraná units is most pronounced for phenocryst-compatible elements (e.g., TiO_2 , FeO, CaO and Sr), which show marked depletions in the Paraná PAV-A and -B units (Fig. 9); other trace elements (e.g., Rb and Th) show little to no variation, and SiO_2 is slightly enriched. These element specific variations and indications for lateral variations in phenocryst content alternatively suggest that a lower degree of geochemical correspondence may result from density segregation of crystals from the pyroclastic density current during flow, which over a run-out distance of >300 km has resulted in detectable fractionation effects in the whole-rock chemistry. Some crystal segregation layering

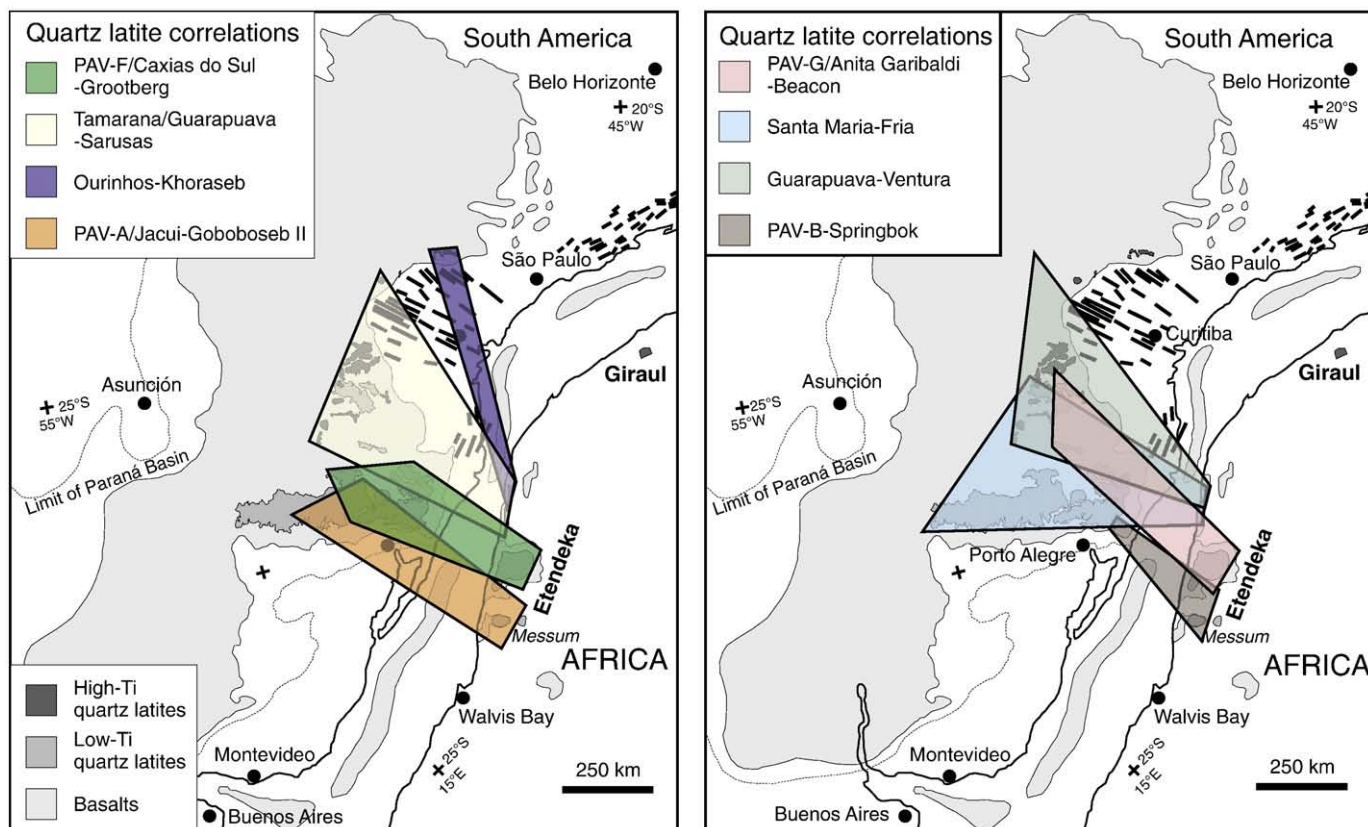


Fig. 7. Map of the pre-rift juxtaposition of South America and Africa showing the Paraná–Etendeka large igneous province (modified from Peate et al., 1992 and Nardy et al., 2008) and the areal extents of correlated silicic eruptive units discussed in text and listed in Table 3. Dashed lines around São Paulo and Curitiba are dyke swarms.

noted by Garland et al. (1995) in Paraná low-Ti (Palmas-type) silicic eruptive units may be a reflection of this flow-induced density segregation. Crystal sorting during run-out has also been suggested for member A of the huge M8.7 Huckleberry Ridge Tuff erupted from Yellowstone caldera at 2 Ma (Christiansen, 2001), suggesting that awareness of this type of process is essential if whole-rock geochemical correlations are attempted for long run-out, large-volume silicic eruptive units.

Table 3 demonstrates that dense rock equivalent eruptive volumes for many large silicic eruptive units in LIPs range between 1000 and 4000 km³ (>M8.5), and are at least equivalent to the dominant erupted volumes for the largest flood basalt lavas from the CRB Province (Table 2). Importantly, the data indicate the Paraná–Etendeka LIP has been the site of up to five silicic eruptions (Table 3) larger in magnitude than the Fish Canyon Tuff (>4500 km³ dense rock equivalent), the most commonly cited example of the largest known ignimbrite eruption (Lipman, 1997; Mason et al., 2004).

In addition to large explosive silicic eruptions, recent studies of the Mesoproterozoic Gawler Range Volcanic Province have delineated three >M8 silicic lava eruptions from this LIP remnant. The large areal extent of these units has been aided by eruptions from multiple point or fissure vents and contemporaneous eruption of chemically distinct magma batches (Allen et al., 2008; McPhie et al., 2008). However, despite similar eruption magnitudes (Table 3), these lavas have run-out lengths that are over an order of magnitude less than the ignimbrite eruptive units. As with basaltic sills intruded into the flood basalt piles, the 2.47 Ga Woongarra Rhyolite sill of the Hammersley Basin in Western Australia (Trendall, 1995) reinforces the point that large-volume batches of silicic magma are emplaced at high stratigraphic levels and available for effusive or explosive eruption

during LIP events. The Woongarra Rhyolite is a composite sill of 15,400 km³ emplaced at depths of a few hundred metres from the paleosurface. Sill emplacement occurred in two pulses thought to be separated by a few hundred years, with the pulses recording injection of 6200 and 9200 km³ of magma (Trendall, 1995).

In terms of cumulative erupted volumes, the silicic LIPs (Bryan et al., 2002; Bryan, 2007; Bryan and Ernst, 2008) contain the largest volumes (~0.25–3 Mkm³) of silicic volcanic rock and are equivalent to many continental flood basalt provinces. Because of this large and rapidly emplaced cumulative volume, the silicic LIPs must also be host to high frequency, large volume (>1000 km³ and >M8) eruptions (Mason et al., 2004; Bryan and Ernst, 2008). However, at present, there are virtually no constraints on the dimensions of individual eruptions from the silicic LIPs. Mid-Tertiary examples from the western USA (e.g., the Fish Canyon Tuff and other monotonous intermediates) give some insight into the potential magnitude of silicic LIP eruptions, as these were erupted at the same time and along strike to the north of the ~0.4 Mkm³ Sierra Madre Occidental silicic LIP, the largest ignimbrite-dominated volcanic province in North America (Swanson et al., 2006; Ferrari et al., 2007). Several examples of similarly crystal-rich and potentially large-volume, caldera-related rhyolitic ignimbrites occur within the Sierra Madre Occidental (e.g., Copper Canyon and Vista Tuffs, Swanson et al., 2006).

5. Discussion

Constraining the dimensions of LIP eruptive units are vital to determining potential rates of magma eruption from vent systems, the duration of eruption and emplacement, and potentially, the rates of magma production and storage (Tolan et al., 1989). This discussion

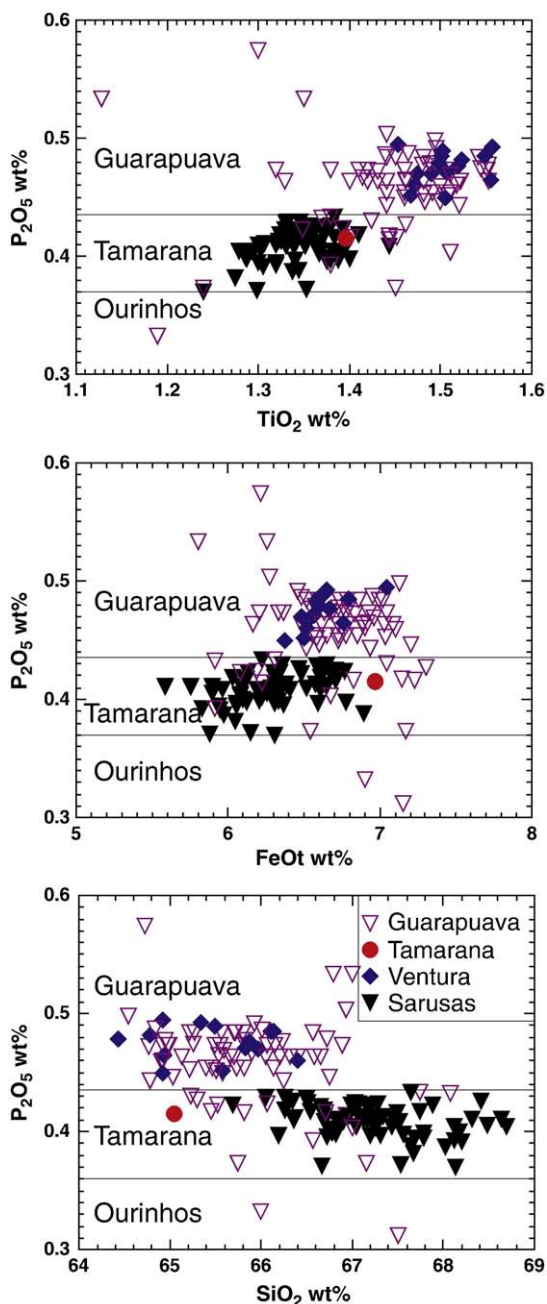


Fig. 8. Discrimination diagrams, in part from Nardy et al. (2008), comparing the Sarusas and Ventura quartz latites from the Etendeka province with the newly defined Guarapuava and Tamarana silicic compositions from the Paraná province.

focuses on these aspects and examines what fundamental differences or similarities exist between the largest basaltic and silicic eruptions.

5.1. Eruption magnitudes of flood basalts vs rhyolites

LIPs have been the site of the largest basaltic and silicic eruptions on Earth (Tables 2 and 3). From the available data on the dimensions of the products of individual eruptions, magma composition does not appear to be a limitation to the upper size limits of erupted magma volume. However, of the larger eruptions, most appear to be 1000–3000 km³, with a few enormous eruptions of 5000 to possibly ≥ 10,000 km³. It is worth noting that given the uncertainty of volume estimations for the silicic eruptive units and the potential for considerable volumes to reside as co-ignimbrite ash deposits, volume

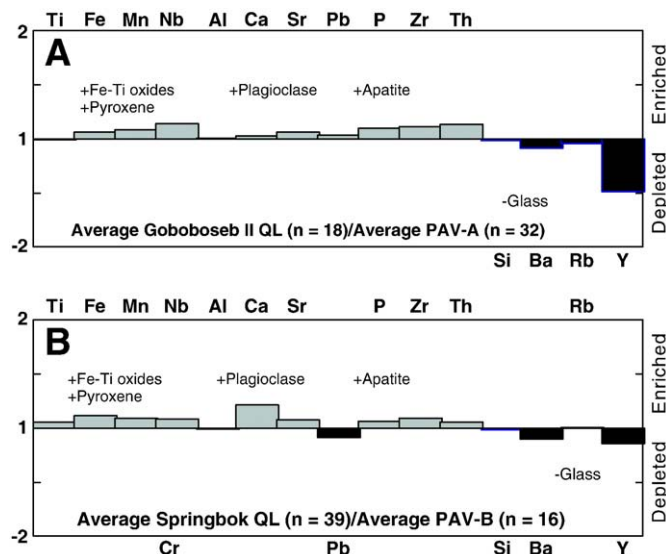


Fig. 9. Enrichment–depletion diagrams showing the variation in major and trace elements for correlated silicic units from the Paraná and Etendeka provinces. In A) the averaged composition of the Etendeka Goboboseb II quartz latite is normalised to the averaged composition of Paraná PAV-A rhyolite (Whittingham, 1991); and in B) the averaged composition of the Springbok quartz latite is normalised to the averaged composition of PAV-B of Whittingham (1991). The Goboboseb and Springbok quartz latites have most likely been erupted from the Messum igneous complex (Ewart et al., 2002) in Namibia suggesting run-out distances of up to ~500 km into the Paraná province. The diagram illustrates subtle geochemical variations between the correlated units, interpreted to represent a proximal to distal chemical variation. For these different eruptions, lateral geochemical variations are similar, with notable depletions in phenocryst-compatible elements, such as Ti, Mn, P and Ca, suggesting that density segregation of phenocrysts during flow over 100s km may have contributed to this chemical variation and produced relatively crystal-poor and ash-enriched deposits in the Paraná. Geochemical data for the Goboboseb II and Springbok quartz latites are from Milner (1988) and Ewart et al. (1998b); data for the PAV-A and PAV-B are from Whittingham (1991); n is number of analyses on which averaged compositions are based.

estimates for silicic eruptive units in LIPs are likely to be considerably underestimated (especially for the Paraná–Etendeka quartz latites). Despite this first-order similarity in the volume of individual eruptions, the basaltic and silicic eruptions are very different in terms of vent types, eruptive mechanisms, magma discharge rates, eruption durations, and emplacement styles (Table 4).

An important consequence for both basaltic and silicic eruptions is that the large magma volume erupted has resulted in eruptive units with long run-out lengths and areal extents. The possible existence of mafic long lava flows up to 1000 km in the Deccan (Self et al., 2008) and on other planets (Keszthelyi et al., 2006) require a large volume of mafic magma in order to satisfy mass continuity, a condition only to be found in LIP eruptions (Self et al., 2008). Likewise, long run-out lengths for pyroclastic density currents emplacing silicic ignimbrite are strongly dependent on a high mass-flux to feed pyroclastic fountaining eruptions (Bursik and Woods, 1996; Freundt, 1999; Branney and Kokelaar, 2002).

5.2. Discharge rates

The two very different vent configurations and eruptive styles (Table 4) play a significant role in the orders of magnitude difference in discharge rates for the basaltic and silicic eruptions in LIPs. For the flood basalt eruptions, early workers inferred fast eruption rates to emplace the huge volumes of magma in a matter of days to a few weeks (Shaw and Swanson, 1970; Swanson et al., 1975; Mangan et al., 1986; Tolan et al., 1989). Determining the discharge rate has obvious implications in terms of the requirement for vast plumbing systems and magma reservoirs for the magma to be delivered quickly to the

Table 4
Summary of the key characteristics of basaltic and silicic eruptions from LIPs. The reader is referred to [White et al. \(2009\)](#) who have summarised the key characteristics of explosive mafic eruptions from LIPs.

Eruption Characteristic	Basaltic Lava Eruptions	Silicic Ignimbrite Eruptions	Silicic Lava Eruptions
Eruptive volumes	Predominantly 100s to 5000 km ³ ; up to 9300 km ³	Predominantly 100s to 5000 km ³ ; up to 9000 km ³	1 to 3000 km ³
Vent-types	Fissures	Calderas, volcano-tectonic rifts/fissures	Point source/domes, fissures
Eruptive styles	Effusive to Hawaiian–Strombolian	Explosive, Plinian to pyroclastic fountaining	Effusive
Magma discharge rates	10 ³ –10 ⁴ m ³ s ⁻¹ ; 10 ³ –10 ⁴ kg s ⁻¹	>10 ⁶ m ³ s ⁻¹ ; 10 ⁹ –10 ¹¹ kg s ⁻¹	?
Eruption Durations	yrs to 10s yr	hours/days to weeks	?
Emplacement Styles	Dominantly pahoehoe lava flow fields	Pyroclastic density currents, fallout from coignimbrite ash plumes; rare plinian fallout	Dominantly non-particulate flow (fluidal to blocky lavas)

surface. The identification of lengthy fissure systems of 70–200 km long in the CRB Province (e.g., [Swanson et al., 1975](#)) provided the mechanism for the rapid evacuation of a huge magma reservoir with the constraint that the mass discharge rate was not so high as to generate a large eruption column. However, the vent system for only one moderate-sized flood basalt eruption (Roza) has been studied in detail, and the nature and extent of activity along other fissure vent systems and dykes for other flood basalt lava flow fields remain poorly known.

The studies of Self and coworkers on the Roza flood basalt eruption have demonstrated that the eruptive volume can be accounted for by an ~10 year duration at an averaged effusion rate of ~4000 m³ s⁻¹ (1.12 × 10⁷ kg s⁻¹), equivalent to the peak rate of the 1783–1784 Laki basaltic eruption in Iceland ([Self et al., 1997](#)). However, given the ~150 km length of the total fissure system for the Rosa flow, at these effusion rates, only part of the fissure system can have been active at any one time. The eruption rate, if averaged over the fissure length, would be exceedingly low (~0.0267 m³/s/m length of fissure) and result in magma freezing in the dykes/fissures in transit to the surface. Such magma freezing may be one mechanism by which effusion becomes concentrated or localised along the fissure system. Voluminous sheet lava flows, therefore, do not require the rapid extrusion of mafic magma at rates much higher than in historic eruptions except for the few cases of young flood volcanism, nor do long fissures imply high eruption rates as only segments of the fissure may be active at any one time (cf. [Hooper et al., 2007](#)).

Many flood basalt lavas in LIPs, were emplaced as inflated pahoehoe sheet flows at effusion rates of 10³–10⁴ m³ s⁻¹ (~2.7 × 10⁶–2.7 × 10⁷ kg s⁻¹). Some flood basalt lavas occur as rubbly pahoehoe flows (e.g., [Self et al., 1997; 1998; Keszthelyi, 2002](#)) where short-lived pulses at higher effusion rates, potentially up to 10⁶ m³ s⁻¹, disrupted the thick, insulating crust and prevented the more commonplace pahoehoe mode of emplacement ([Keszthelyi et al., 2006](#)). One explanation is that these surges of higher effusion rate may reflect enhanced periods of magma effusive activity over greater lengths of the fissure system ([Brown and Self, 2008](#)).

The potential similarity in terms of discharge rate and therefore eruption style between small-volume historic (<20 km³; e.g., Laki) and flood basalt (≥1000 km³) eruptions raises the possibility that there is a physical limitation to how much, and how quickly, basaltic magmas can be erupted. Despite the length of fissure vents, the effusion rates appear supply rate-constrained, resulting in eruptions that must last years to 10s years to empty any stored magma reservoirs despite their size. An insight into why flood basalt eruptions do not have extraordinarily high discharge rates given the huge volumes of magma erupted may come from temporal compositional trends observed in smaller volume intraplate basalt eruptions ([Reiners, 2002](#)). In these cases, rates of melt extraction from the mantle and source-to-surface melt velocities of ~10⁰–10¹ km/yr are indicated, and may provide one limiting constraint on effusion rate at the vent for the most primitive flood basaltic magmas with little evidence for crustal storage, assimilation or fractionation. However, most flood basalt magmas require significant residence at crustal

levels, given their compositions are not primitive (e.g., [Cox, 1980](#)), and buoyancy forces or high magma densities represent the main constraint on chamber evacuation and eruption rates.

Few constraints are available for discharge rates of silicic eruptions during LIP events. This is in part due to the lack of information on the nature of source vents and the virtual absence of plinian fall deposits in LIPs from which most constraints on magma discharge rates for silicic explosive eruptions are made (e.g., [Wilson et al., 1978; Sparks, 1986; Wilson and Walker, 1987; Carey and Sigurdsson, 1989](#)). The large-volume silicic eruptive units in LIPs are dominantly ignimbrite or rheoignimbrite (e.g., [Milner et al., 1992; Bryan et al., 2002; Ukstins Peate et al., 2005; Bryan, 2007](#)) and the general lack of widespread plinian fall deposits suggest that in general, mass discharge rates are sufficiently high (>10⁸–10⁹ kg/s) to prevent stable and buoyant plinian eruption columns forming at the onset of, and during eruptions. Other factors that would contribute to co-current eruption dynamics include large, wide or multiple vents, such as fissures or along ring faults, and lower gas content (particularly for the rheomorphic ignimbrite examples) that in turn help lower eruption velocity ([Wilson et al., 1980; Woods, 1995; Freundt, 1999](#)). In general, the formation of single cooling units and in some cases, absence of internal erosion surfaces or sedimentary deposits produced by epiclastic processes within ignimbrite sheets have been interpreted to indicate ignimbrite emplacement within a period of no more than a few hours or days (e.g., [Christiansen, 1979; 2001](#)).

The inferred intensities for a number of prehistoric and historic plinian eruptions vary between 1.6 × 10⁶ kg s⁻¹ and 1.1 × 10⁹ kg s⁻¹ ([Carey and Sigurdsson, 1989](#)), whereas the magma discharge rate for the June 15, 1991 eruption of Mt Pinatubo was between 4 × 10⁸ and 2 × 10⁹ kg s⁻¹ ([Koyaguchi, 1996](#)). Assuming a discharge rate of 1 × 10⁹ kg s⁻¹ and given the deposit volumes of the large silicic eruptive units in [Table 3](#), the estimated duration of these eruptions varies from ~44 days for the smallest volume ignimbrite listed (Sana'a Ignimbrite, Afro-Arabian LIP) to ~248 days for the Guarapuava-Tamarana/Sarasus quartz latite (Paraná–Etendeka LIP). If mass eruption rates were an order of magnitude lower, then eruption durations would be in the order of 1–10 years, and approach the inferred durations of the flood basalt lava eruptions. The duration of the first pulse of the Woongarra Rhyolite sill emplacement has been estimated at ~240 years, equating to a magma discharge rate of 5 × 10⁶ kg s⁻¹ ([Trendall, 1995](#)), which approaches discharge rates of Quaternary sub-plinian eruptions ([Carey and Sigurdsson, 1989](#)). In such long-lived eruptions, we would expect to see unsteadiness in the eruption that would be reflected in bedding or multiple eruptive units in the deposits, which are rarely observed (cf. Sarasus quartz latite, [Ewart et al., 2004b](#)). Alternatively, if eruption durations approach those from well-documented Quaternary eruptions (i.e. hours to days), then eruption intensities of 10¹⁰ to 10¹¹ kg s⁻¹ are required. Such high eruption intensities without the development of a tall Plinian eruption column can be achieved by multiple vents or ring fracture fissure eruptions. The simple deposit structures of the silicic eruptive units thus supports the notion for high eruptive fluxes (10⁹–10¹¹ kg s⁻¹) and short duration (<1 month) eruptions. These higher

rates are supported by recent work on giant ash clouds (Baines and Sparks, 2005) that suggest eruption intensities approach $10^{10} \text{ kg s}^{-1}$ resulting in durations between 2 and 10 days for the largest eruptions (M8–9). Additional supporting examples for short durations include the 450 km³ Bishop Tuff eruption from Long Valley, California, about 770,000 years ago that has been estimated to have lasted about 4 days (Wilson and Hildreth, 1997), and the compositionally zoned 2200 km³ Huckleberry Ridge Tuff erupted from the Yellowstone volcanic field, which occurs as a single cooling unit and likewise been suggested to result from an eruption that took days at most (Christiansen, 1979, 2001).

5.3. Frequency of large-magnitude (>M8) eruptions from LIPs

It is both the volume of magma emitted during individual eruptions in LIP events and the total volume of magma released (>0.1–80 Mkm³) that make LIP events so exceptional in Earth history (Self et al., 2005; Self, 2006). It is this combination of large erupted volumes and high frequency that lead to the rapid construction of thick (1–3 km) areally extensive plateaus (0.1–2 Mkm²), which internally, show few signs of major time breaks, erosion surfaces and regional unconformities (Fig. 6A). The high-frequency of large-magnitude eruptions also distinguishes LIP events from other tectonic settings and processes where igneous rocks are formed. Importantly, without LIP-forming igneous events, basalt super-eruptions would not have occurred through Earth history, but in contrast, silicic super-eruptions have occurred independently of LIP events (Sparks et al., 2005).

From a volcanological viewpoint, geochronological studies of LIPs, summarized in studies such as Rampino and Stothers (1988), Courtillot and Renne (2003), Kelley (2007), Bryan and Ernst (2008) and Chenet et al. (2008), have revealed two main features relevant to the timing of eruptions and LIP formation. These are that: 1) much (70–90%) of the eruptions are produced during one or two main pulses of eruptive activity; and 2) that the pulse or pulses, or even the whole duration of activity in the LIP, can be very brief geologically, <5 Ma, and possibly even <1 Ma in some cases. For LIPs of any age, the errors on the age estimates cannot resolve individual formations within these pulses of activity, and certainly cannot resolve individual eruptions. In many cases, the errors encompass the age range of almost all eruptive units from top to bottom of the LIP pile (e.g., Barry et al., 2010).

For the flood basalt eruptions, evidence from the CRB LIP suggests that during the main pulse and emplacement of the Grande Ronde and Wanapum Basalt Formations (~16.5–15.3 Ma), a high frequency of the largest magnitude eruptions existed producing the most voluminous flow fields (Tolan et al., 1989). For example, the Grande Ronde Basalt forming >60% of the total volume of the CRB LIP (Camp et al., 2003; Barry et al., 2010) with an average volume of 1238 km³ (Tolan et al., 1989). New ⁴⁰Ar/³⁹Ar dates for Grande Ronde lavas reveal they were emplaced within a maximum time range of 0.42 ± 0.18 Myr (Barry et al., 2010), corresponding to an averaged frequency of \geq M8 eruptions of 220/Myr or one \geq M8 eruption every ~4200 yr. For larger continental flood basalt provinces such as the Deccan, recent studies (Self, 2006; Self et al., 2008; Chenet et al., 2009) indicate that individual formations emplaced over similar time scales of hundreds of thousands of years, have volumes either equivalent to the main phase lavas (Grande Ronde Formation, ~0.15 Mkm³) or to the entire CRB LIP (~0.23 Mkm³, Camp et al., 2003). Therefore, LIP formations must be characterised by even higher frequencies of M8 and larger eruptions.

For most LIPs other than the CRB, however, the number of eruptions is unknown. Even within the CRB, the number is not known precisely but is probably around 200. Fitting the number of eruptions within a 1–2 Ma timeframe still gives average eruption intervals of 1000 s–10,000 yr (Self et al., 2006; Barry et al., 2010). While the

accumulated lava pile, and the thickness added by each eruption, is impressive, considered from a modern or historic perspective, LIP eruptions probably were not necessarily 'hyperactive', even during the main pulse. Much more needs to be known about the rates of lava production and the lengths of hiatuses between eruptions in LIPs, and various approaches are being undertaken to estimate this (Chenet et al., 2008; Jolley et al., 2008), but such studies are in their infancy.

The recent compilation on large-volume silicic explosive eruptions by Mason et al. (2004) revealed 42 known eruptions of >M8 over the past 36 Ma. This yielded a minimum time-averaged estimate of eruption frequency of 1.1 events/Myr since the beginning of the Oligocene, but over this time, such large magnitude eruptions have clustered in two pulses at 36–25 Ma and 13.5 Ma to present. The older pulse corresponds to two LIP events: the Afro-Arabian and Sierra Madre Occidental provinces but with most dimensional data for eruptions drawn from related large-volume silicic ignimbrite volcanism to the north of the Sierra Madre Occidental in the Great Basin region of western U.S.A. (e.g., Gans et al., 1989; Best and Christiansen, 1991). During these pulses, large eruption frequencies were slightly higher at ~2 events/Myr. However, virtually no data are currently available on the magnitude of individual silicic eruptions within the Sierra Madre Occidental, and >M8 eruption frequencies will have been much higher for this period. In contrast to the eruptive record for the last 35 Myrs, large eruption frequencies were at least 9 events/Myr during the Parana–Etendeka LIP event, and for the Afro-Arabian province, the equivalent of 12 events/1 Myr. Consequently, the frequency of silicic super-eruptions is greater during LIP events than when compared to global, long-term averaged frequencies of silicic super-eruptions. Importantly though, based on available age data for the continental flood basalt provinces, these high frequencies are sustained only for very brief periods of \leq 1 Myr.

5.4. Generation and storage of large magnitude LIP eruptions

The eruption of such exceptionally voluminous magmas and the often remarkable chemical homogeneity in on-land deposits have led to the general interpretation that LIP eruptions require very large magma reservoirs, which are rapidly evacuated. The very large volumes for individual eruptions from LIPs raise a number of space-volume issues in terms of the storage and dimensions of, and connectivity and interactions between holding chambers within the crust. As noted by Ewart et al. (1998b), the erupted volume of the Springbok quartz latite equates to a magma sphere diameter of 23 km. Alternatively, a sill-like magma body with dimensions of $\sim 4 \times 40 \times 40$ km also approximates the minimum erupted volume of the Springbok quartz latite. The Messum igneous complex, identified as the eruptive centre for the Springbok quartz latite (Milner and Ewart, 1989) is a roughly circular structure of ~18 km diameter, but is characterised by down-sagging margins and inward-dipping strata following the quartz latite eruptions (Ewart et al., 2002). Volumetric considerations suggest that chamber dimensions were much greater than the collapse diameter of Messum, hence resulting in regional down-sagging rather than classical Valles-type caldera collapse structures (see also Volcan de l'Androy, Madagascar LIP; Mahoney et al., 2008). The lack of well-defined calderas in LIPs may thus be in part due to the greater depth and lateral dimensions of the magma chambers.

Not only do issues of space arise from the storage of such huge volume magma bodies in the crust, but additional complications arise in a temporal sense because many >M8 basaltic and silicic eruptions may occur within 1 Myrs, some or all of which may be genetically unrelated and represent new episodes of large-volume magma generation. For example, a number of large volume (>1000 km³), closely-spaced ($\leq 10^5$ yr) and genetically related silicic eruptions (Goboboseb and Springbok quartz latites) occurred from the Messum igneous complex, and which overlapped in space and time with flood

basaltic eruptions (Ewart et al., 1998b; 2002). How do these magma reservoirs spatially overlap and how does this impact on the thermal and rheological character (e.g., de Silva and Gosnold, 2007) of the crust? The architecture and spatial-temporal relationships of flood basaltic and rhyolitic magma reservoirs in the crust during LIP events remain poorly understood.

Considerable petrographic and chemical evidence indicates that many flood basaltic magmas underwent storage, fractional crystallisation and crustal assimilation at lower crustal pressures prior to eruption (Cox, 1980; Hooper, 1997; Ewart et al., 1998a; Ramos et al., 2005; Hooper et al., 2007), as well as potentially further storage, fractionation and degassing at shallow depths in sill complexes prior to final extrusion (e.g., Cox, 1980; Rodriguez Durand and Sen, 2004; Puffer et al., 2009). However, the lack of caldera collapse structures associated with flood basalt magma withdrawal implies that any reservoirs were most likely located at middle to lower crustal depths (Hooper, 1997) or that magma is both intruded into and inflating, rather than evacuating shallow-level sills while also being extruded at the surface (Puffer et al., 2009). In contrast, some flood basalt lavas show little evidence for crustal storage or assimilation and retain primitive mantle geochemical and isotopic signatures (e.g., Tafelkop and Santa Lucia basalts, Paraná–Etendeka Province, Ewart et al., 1998a; Kirstein et al., 2000). Although these magmas can be interlayered with the more common fractionated basaltic magmas, they must have a different transport history and pathway from mantle source regions to the surface.

While LIPs often show evidence for bimodality and a prominent silica or Daly gap, recent studies of the Paraná–Etendeka and Afro-Arabian LIPs have revealed the presence of more intermediate magma compositions (Ewart et al., 2004b; Ukstins Peate et al., 2008) that reduce the significance of the compositional gap between the associated flood basalts and rhyolites. For the Paraná–Etendeka province, intermediate (latite) compositions are small in volume and restricted in distribution that have hindered their recognition, but they are significant in establishing petrogenetic linkages between the associated flood basalt and rhyolitic magmas (e.g., Ewart et al., 2004b). In contrast, it is in distal tephra records to the Afro-Arabian LIP that a more complete compositional spectrum of LIP magmas is recorded. Tephra from the Indian Ocean (~3000 km away), which have been temporally, geochemically, isotopically, and paleomagnetically correlated to individual silicic eruptions in Yemen and Ethiopia, preserve a complete spectrum of compositions ranging from basalt (43 wt.% SiO₂) to rhyolite (75 wt.% SiO₂) in individual tephra shards from within a single eruption (Ukstins Peate et al., 2008). In addition, banded shards from individual eruptions record up to 85% of the SiO₂ variation observed in the entire eruption at the scale of <1 mm³, clearly demonstrating that the entire magmatic compositional variation found within a LIP can potentially be sampled by individual eruptive events. This requires that the full spectrum of compositions, representing an extreme range from basaltic through silicic, may be present within magma chambers at the time of eruption, and argues for magma chamber connectivity, efficient evacuation and large as well as small-scale mingling and mixing during eruption.

Many documented large-volume (>1000 km³) silicic eruptions in the recent geologic record are examples of crystal-rich (30–50%) dacite–rhyolites labelled as “monotonous intermediates” by Hildreth (1981), including four of the largest eruptions occurring since 35 Ma listed by Mason et al. (2004): the Fish Canyon Tuff (an archetypal monotinous intermediate), Toba Tuff, Lund Tuff and Atana Ignimbrite. Recent studies of the Fish Canyon Tuff by Bachmann et al. (2002, 2005) recognised that this and other crystal-rich silicic ignimbrites record the eruption of batholithic volumes of crystal mush forming in upper crustal magma chambers. Whereas the rejuvenated batholith model (e.g., Bachmann and Bergantz, 2003, 2006, 2009) satisfactorily explains the essential features of the large-volume “monotonous intermediates”, this genetic model cannot be applied to the similarly

large and larger-volume rhyolite eruptions from the continental flood basalt provinces. Voluminous deposits of crystal-rich ignimbrites (i.e. monotinous intermediates) for example, are absent from the continental flood basalt provinces, and Streck and Grunder (2008) have provided other arguments against mush extraction models for high-temperature, crystal-poor Fe-rich rhyolites. Many LIP rhyolites are distinguished by their large volume, crystal-poor nature, anhydrous mineralogy, high crystallisation and eruption temperatures (>1000 °C) and strong geochemical evidence for a petrogenetic link with associated flood basalts (Bellieni et al., 1986; Garland et al., 1995; Peate, 1997; Ewart et al., 1998b; 2004b; Ukstins Peate et al., 2008). An alternative model for the origin of these large-volume crystal-poor LIP rhyolites is thus required.

We consider that the variety of large-volume basaltic and silicic eruptions in LIPs can be envisaged in terms of four end-member magma petrogenetic pathways (Fig. 10). Certain flood basaltic magmas preserve mantle geochemical signatures and show little to no evidence for storage at crustal depths, low pressure crystallisation and crustal assimilation. These smaller volume flood basaltic magmas may have been transferred directly from melting regions in the upper mantle to fissure vents at surface or have resided temporarily in reservoirs in the upper mantle or in mafic underplate, thereby preventing opportunities for crustal contamination (pathway A in Fig. 10). In contrast, it is more common for the larger volume flood basaltic magmas (notably low-Ti types) to have undergone storage at lower ± upper crustal depths resulting in crustal assimilation, crystallisation, and degassing to produce aphyric to plagioclase-dominant basaltic and basaltic andesite lavas (pathways B1 and B3 in Fig. 10). Large volume high-Ti-type flood basalts (e.g., Khumib–Urubici-type, Peate et al., 1999; Ewart et al., 2004a) also show evidence for crustal storage and shallow-level fractionation prior to eruption but have not undergone significant (silicic) crustal assimilation (pathway B2 in Fig. 10).

For the crystal-poor large-volume rhyolites in continental LIPs, most workers have invoked large-scale AFC processes involving lower crustal granulite melting and/or remelting of basaltic underplate with additional mafic and silicic magma inputs and extended fractional crystallisation (pathway C in Fig. 10) to generate the high-temperature anhydrous, crystal-poor silicic magmas characteristic of LIPs such as the Paraná–Etendeka and Karoo (e.g., Piccirillo et al., 1987; Garland et al., 1995; Ewart et al., 1998b, 2004b; Miller and Harris, 2007). Surface expressions of these eruptions may be regional sag structures (Ewart et al., 2002) or fissure vents, with well-defined surface calderas absent due to high-temperature (>1000 °C) magma reservoirs residing at deeper crustal levels. Chambers at mid to lower crustal levels are more likely to lack chilled envelopes or sidewall crystallisation and undergo strong convective mixing promoting chemical homogenisation.

Large-volume, lower temperature (<900 °C) crystal-rich rhyolite ignimbrites, as found in the silicic LIPs (Bryan, 2007) and extensional continental margin environments (e.g., Altiplano Puna province), appear to have an origin similar to that described for the Fish Canyon Tuff and other ‘monotonous intermediate’ ignimbrites. In these cases, the eruptions reflect remobilisation of near-solidus magmatic mushes or magma bodies of several thousands of km³ (with ~45–50 vol.% crystals) that are in the process of forming upper-crustal batholiths (pathway D1 in Fig. 10). Shallow intrusion and underplating by basaltic mafic magmas, which can be enhanced by active extension (Ferrari et al., 2009) provide the necessary thermal and volatile inputs to trigger the eruption of these upper crustal chambers and the development of well-defined calderas up to 80 km in diameter. By contrast, upper crustal intrusion of basalt also leads to the rapid generation and eruption of moderate volumes of crystal-poor rhyolite through the remelting of solidified and highly differentiated plutonic rocks formed during preceding phases of magmatism in the LIP event (pathway D2 of Fig. 10), and the Alacrán ignimbrite (Bryan et al.,

- A. Primitive, mantle-dominated basalt lavas**
 eg. Tafelkop-Santa Lucia lavas
 Paraná-Etendeka
- Direct transfer of magma from melting regions or temporary storage zones in upper mantle to fissure vents at surface. Little to no storage at crustal levels or crustal contamination of magmas. Eruption rate may be melt generation and transfer rate-limited. Eruption of low- to moderate-volume, mildly alkaline to tholeiitic and commonly olivine-phyric lavas.
- B. Large-volume flood basaltic lavas**
 eg. Tafelberg-Gramado & Khumbi-Urubici lavas
 Paraná-Etendeka
- Sills of mantle-derived magmas injected at crust-mantle interface. B1: lower crustal assimilation, fractional crystallisation and mafic magma recharge. B2: basaltic intrusion within mafic underplate inhibits crustal contamination with petrogenetic processes dominated by fractional crystallisation and magma mixing ± partial melting of basaltic underplate. Rapid melt extraction to surface also limits crustal contamination. B3: mid and upper crustal storage results in further crustal assimilation, crystallisation and magma degassing. Sustained dyke/fissure-fed eruptions of large-volume aphyric to plagioclase-augite-phyric basalts and basaltic andesites.
- C. Large-volume high-temperature rhyolites**
 eg. Springbok, Sarusas quartz latites, Paraná-Etendeka; SAM ignimbrite, Afro-Arabian
- Two petrogenetic lineages reflecting major (low-Ti, C1) and minimal (high-Ti-type magmas, C2) crustal involvement. C1: lower crustal melting and assimilation in response to basaltic underplating with further mafic recharge; crustal melting fusion fronts may migrate upwards over time. Further mid to upper crustal storage with assimilation of granitic-type crustal materials and fractional crystallisation. C2: ponding and fractionation or remelting of high-Ti-type basalts near crust-mantle boundary with further mafic magma recharge; any storage at mid crustal levels may promote silicic magma mixing or contamination resulting from crustal assimilation or interaction with unroofed silicic magmas. Eruption of high-temperature (>950 °C) anhydrous, plagioclase-pyroxene-phyric, weakly to unzoned magma batches; Regional sag structures and lack of well-defined surface calderas due to magma reservoirs residing at deeper crustal levels, having a large lateral extent and/or fissure eruptions.
- D. Large volume low-temperature rhyolite ignimbrites**
 eg. Fish Canyon, Vista, Alacrán Tuffs
 Sierra Madre Occidental, silicic LIPs
- Silicic magma source zones in mid to upper crust developed in response to shallow intrusion of mafic magmas providing thermal, mass and volatile inputs (gas sparging). D1: rejuvenation of near-solidus upper-crustal batholiths (mainly crystal mush) by intruded and underplated basaltic magma, leading to eruption of large-volume crystal-rich (30–50%), dacitic to rhyolitic magmas (e.g., Fish Canyon Tuff). D2: remelting of earlier formed and solidified plutons resulting in the rapid generation and eruption of moderate volume, crystal-poor and anecrystic silicic magma (e.g., Alacrán Tuff). Well-defined surface calderas (20–80 km diameter) or volcanotectonic collapse structures where eruptions are fissure-fed.

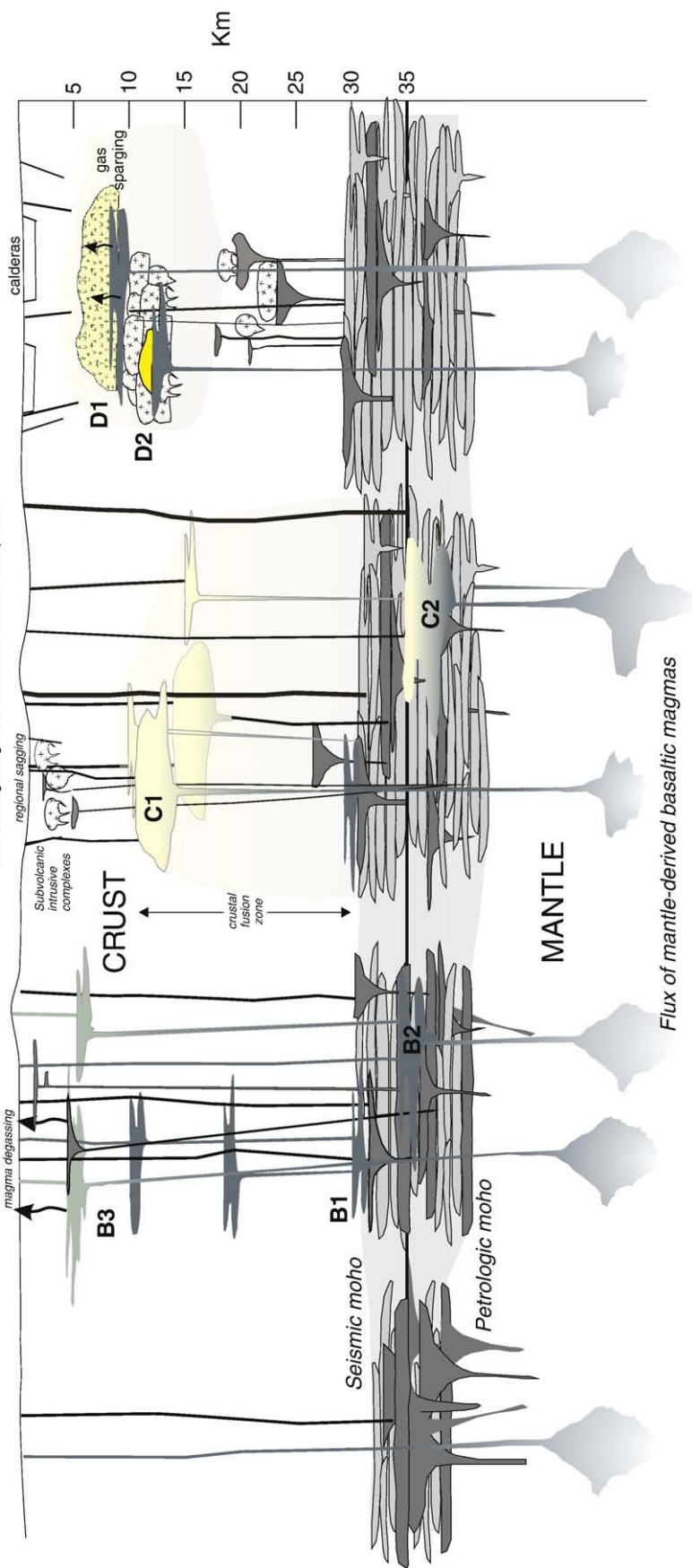


Fig. 10. Conceptual crustal view (not to horizontal scale) of four end-member petrogenetic pathways for large magnitude (basaltic and silicic) eruptions, principally in continental LIPs. The effects of crustal thinning on magma generation are not included in this depiction. Sills of mantle-derived basaltic magma are injected principally near the crust-mantle boundary. Over time this underplated basaltic magma produces seismic (top of basaltic underplate) and petrologic (base of underplate) mohos. Basaltic magmas may be either (A) extracted rapidly from melting source regions in the mantle and erupted at the surface, or (B) pond in lower crustal magma chambers where the magmas become subject to open system processes (assimilation, magma mixing, melt extraction) as well as fractional crystallisation. Low-Ti-type flood basalt magmas (B1; e.g., Tafelberg-Gramado lavas, Ewart et al., 1998a) have typically experienced assimilation of intermediate to silicic composition lower crust, whereas high-Ti-type flood basalt magmas (B2; e.g., Khumbi-Urubici lavas, Ewart et al., 2004a) have typically experienced magma mixing ± remelting of the newly formed underplate. In both cases, additional upper crustal storage (B3) can result in further crustal assimilation, crystallisation and magma degassing. High-temperature (>950 °C) silicic magmas are genetically related to the low- and high-Ti type flood basaltic magmas and large-scale crustal assimilation characterises low-Ti (C1) silicic magmas (e.g., Goboboseb and Springbok quartz latites, Ewart et al., 1998b), whereas high-Ti silicic magmas (C2) show little to no evidence for the involvement of silicic crust in their petrogenesis (e.g., Chapeco-type rhyolites, Garland et al., 1995; Ewart et al., 2004b), and appear to be rapidly extracted from magma chambers residing in the lower crust. Thermal and mass fluxes of basalts to mid to upper crustal depths result in either the remobilisation of felsic cumulate piles or partially crystallised batholiths (D1) akin to the model for the Fish Canyon Tuff proposed by Bachmann et al. (2002). Additionally, remelting of differentiated and solidified granitic intrusions (D2, e.g., Alacrán Tuff of the Sierra Madre Occidental, Bryan et al., 2008) can also occur, producing moderate to large volumes of relatively low-temperature (<850 °C), high-K₂O rhyolites.

2008) in the Sierra Madre Occidental silicic LIP is an example of this petrogenetic pathway.

6. Conclusions

Large igneous provinces have been the loci for both basaltic and silicic super-eruptions (>M8) throughout Earth history, and are therefore important for understanding their potential for driving environmental and climate change and causing mass extinctions, melt production rates from the sublithospheric mantle and crust, the thermal, mechanical and compositional evolution of the lithosphere, and what upper limits there may be to the volume and rate of magma eruption. LIPs are unique for their substantial cumulative volumes (>10⁵–10⁷ km³) of emplaced magma over brief periods (1–5 Myrs) that ultimately results from 10s to 100s of >M8 eruptions and intrusions. The compilation here indicates that basaltic and silicic super-eruptions from LIPs have similar magnitudes, but the difficulties in identifying co-ignimbrite ashes for the silicic eruptive units result in present volumes being significant underestimates. Nevertheless, magma composition appears to be no barrier to the volume of magma erupted, and several basaltic and silicic super-eruptions from LIPs are estimated to have been >M9.2, and consistent with a calculated upper limit to eruption size by Mason et al. (2004). Based on the data set presented here and that of Mason et al. (2004), it appears that an upper limit of ~M9 exists for other tectonic settings, but for LIPs a more realistic upper limit of eruption magnitude is closer to M9.5 (or ~11,000 to 12,000 km³ of magma). Supply rate and duration seem to be the primary factors controlling the run-out length, areal extent and volume of the basaltic and silicic eruptive units. These basaltic and silicic super-eruptions do significantly differ in terms of eruptive frequency, sources, style and emplacement mechanisms, but have petrogenetic linkages. The dominantly effusive nature and lower discharge rate (10⁶–10⁸ kg s⁻¹) for the basaltic super-eruptions are inferred to result in long durations (yrs to >10 yr) for individual eruptions, which in some cases may be a melt generation rate-limited process. In contrast, the deposit characteristics of silicic super-eruptions in LIPs suggest very high-rate (10⁹–10¹¹ kg s⁻¹), short-lived eruptions, similar to eruption durations of hours to days for well-studied Quaternary eruptions; such eruptive rates require the availability of 1000s km³ of silicic magma stored in crustal chambers to be erupted. Importantly, detailed studies of LIPs are revealing evidence for the contemporaneous interaction and eruption of basaltic and silicic magmas, which challenges concepts of how and where in the lithosphere such large volumes of magma are stored and what pathways they utilise to erupt at the surface. Further studies are required to rigorously establish eruptive unit correlations for all LIPs, and linking onshore silicic eruptive units with distal and marine-deposited co-ignimbrite ash deposits that will give considerable insight into the eruptive mechanisms, global ash dispersion (e.g., Peate, 2009), and environmental effects from individual or successive, closely-spaced large magnitude (>M8) super-eruptions.

Acknowledgements

Simon Milner, Andy Duncan, Richard Ernst, Luca Ferrari, Alexei Ivanov and particularly Tony Ewart are thanked for extensive discussions on aspects of this manuscript. Scott Bryan acknowledges support from Kingston University, and Ingrid Ukstins Peate and David Peate acknowledge support from NSF grant EAR0439888 for this work. Additional support has been provided by National Research Foundation (South Africa) grant FA2006032400017 to Jodie Miller, Chris Harris & Scott Bryan. Namibia fieldwork was supported by the Geological Survey of Namibia, and AAPG (Gustav E. Archie Fund) and Geological Society of London (Elspeth Matthews Grant) awards to Mike Mawby. David Pyle and Martin

Menzies are thanked for supportive and constructive reviews of the manuscript.

References

- Allen, S.R., McPhie, J., 2002. The Eucarro Rhyolite, Gawler Range Volcanics, South Australia: An 675 km³ compositionally zoned felsic lava of Mesoproterozoic age. *Geological Society of America Bulletin* 114, 1592–1609.
- Allen, S.R., Simpson, C.J., McPhie, J., Daly, S.J., 2003. Stratigraphy, distribution and geochemistry of widespread felsic volcanic units in the Mesoproterozoic Gawler Range Volcanics, South Australia. *Australian Journal of Earth Sciences* 50, 97–112.
- Allen, S.R., McPhie, J., Ferris, G., Simpson, C., 2008. Evolution and architecture of a large felsic Igneous Province in western Laurentia: The 1.6 Ga Gawler Range Volcanics, South Australia. *Journal of Volcanology and Geothermal Research* 172, 132–147.
- Bachmann, O., Bergantz, G.W., 2003. Rejuvenation of the Fish Canyon magma body: A window into the evolution of large-volume silicic magma systems. *Geology* 31, 789–792.
- Bachmann, O., Bergantz, G.W., 2006. Gas percolation in upper-crustal silicic crystal mushes as a mechanism for upward heat advection and rejuvenation of near-solidus magma bodies. *Journal of Volcanology and Geothermal Research* 149, 85–102.
- Bachmann, O., Bergantz, G.W., 2009. Rhyolites and their source mushes across tectonic settings. *Journal of Petrology* 49, 2277–2285.
- Bachmann, O., Dungan, M.A., Lipman, P.W., 2002. The Fish Canyon magma body, San Juan volcanic field Colorado; rejuvenation and eruption of an upper-crustal batholith. *Journal of Petrology* 43, 1469–1503.
- Bachmann, O., Dungan, M.A., Bussy, F., 2005. Insights into shallow magmatic processes in large silicic magma bodies: the trace element record in the Fish Canyon magma body, Colorado. *Contributions to Mineralogy and Petrology* 149, 338–349.
- Baines, P.G., Sparks, R.S.J., 2005. Dynamics of giant volcanic ash clouds from supervolcanic eruptions. *Geophysical Research Letters* 32 (24), L24808 doi:10.1029/2005GL024597.
- Barker, P.R., Kennett, J.P., et al., 1988. Sites 691 and 692. *Proceedings of the Ocean Drilling Project, Initial Reports*, 113: College Station, TX (Ocean Drilling Program).
- Barry, T., Self, S., Kelley, S.P., Hooper, P., Reidel, S.P., Hooper P., Widdowson, M., 2010. New ⁴⁰Ar/³⁹Ar dating of the Grande Ronde lavas, Columbia River Basalts, USA: implications for duration of flood basalt eruption episodes. *Lithos* 118, 213–222.
- Beeson, M.H., Fecht, K.R., Reidel, S.P., Tolan, T.L., 1985. Regional correlations within the Frenchman Springs Member of the Columbia River Basalt Group; new insights into the middle Miocene tectonics of northwestern Oregon. *Oregon Geology* 47, 87–96.
- Bell, B.R., Emeleus, C.H., 1988. A review of silicic pyroclastic rocks of the British Tertiary Volcanic Province. In: Morton, A.C., Parson, L.M. (Eds.), *Early Tertiary volcanism and the opening of the NE Atlantic: Geological Society of London Special Publication*, vol. 39, pp. 365–379.
- Bellieni, G., Comin-Chiaromonti, P., Marques, L.S., Melfi, A.J., Nardy, A.J.R., Papatrechas, C., Piccirillo, E.M., Roisenberg, A., Stofa, D., 1986. Petrogenetic aspects of acid and basaltic lavas from the Paraná Plateau (Brazil): geological, mineralogical and petrochemical relationships. *Journal of Petrology* 27, 915–944.
- Best, M.G., Christiansen, E.H., 1991. Limited extension during peak Tertiary volcanism, Great Basin of Nevada and Utah. *Journal of Geophysical Research* 96, 13,509–13,528.
- Bonadonna, C., Ernst, G.G.J., Sparks, R.S.J., 1998. Thickness variations and volume estimates of tephra fall deposits: the importance of particle Reynolds number. *Journal of Volcanology and Geothermal Research* 81, 173–187.
- Bondre, N.R., Duraiswami, R.A., Dole, G., 2004. Morphology and emplacement of flows from the Deccan Volcanic Province. *Bulletin of Volcanology* 66, 29–45.
- Branney, M.J., Kokelaar, P., 1992. A reappraisal of ignimbrite emplacement: progressive aggradation and changes from particulate to non-particulate flow during emplacement of high-grade ignimbrite. *Bulletin of Volcanology* 54, 504–520.
- Branney, M.J., Kokelaar, B.P., 2002. Pyroclastic density currents and the sedimentation of ignimbrites. *Geological Society of London Memoirs* 27, 1–152.
- Branney, M.J., Bonnicksen, B., Andrews, G.D.M., Ellis, B., Barry, T.L., McCurry, M., 2008. 'Snake River (SR)-type' volcanism at the Yellowstone hotspot track: distinctive products from unusual, high-temperature silicic super-eruptions. *Bulletin of Volcanology* 70, 293–314.
- Bristow, J.W., 1976. The geology and geochemistry of the southern Lebombo. MSc thesis, University of Natal, Durban, 331 pp.
- Brown, R., Self, S., 2008. Vent complexes and eruptive mechanisms of the Roza basalt flow field, Columbia River Basalt province. *EOS. Transactions of the American Geophysical Union* 89 (53) (Fall Meeting Supplement, Abstract V53A-2120).
- Bryan, S.E., 2007. Silicic Large Igneous Provinces. *Episodes* 30, 20–31.
- Bryan, S.E., Ernst, R.E., 2008. Revised definition of Large Igneous Provinces (LIPs). *Earth Science Reviews* 86, 175–202.
- Bryan, S.E., Constantine, A.E., Stephens, C.J., Ewart, A., Schön, R.W., Parianos, J., 1997. Early Cretaceous volcano-sedimentary successions along the eastern Australian continental margin: Implications for the break-up of eastern Gondwana. *Earth and Planetary Science Letters* 153, 85–102.
- Bryan, S.E., Riley, T.R., Jerram, D.A., Leat, P.T., Stephens, C.J., 2002. Silicic volcanism: an under-valued component of large igneous provinces and volcanic rifted margins. In: Menzies, M.A., Klemperer, S.L., Ebinger, C.J., Baker, J. (Eds.), *Magmatic Rifted Margins: Geological Society of America Special Paper*, 362, pp. 99–120.
- Bryan, S.E., Ferrari, L., Reiners, P.W., Allen, C.M., Petrone, C.M., Ramos Rosique, A., Campbell, I.H., 2008. New insights into crustal contributions to large volume rhyolite generation at the mid-Tertiary Sierra Madre Occidental Province, Mexico, revealed by U–Pb geochronology. *Journal of Petrology* 49, 47–77.

- Bursik, M.I., Woods, A.W., 1996. The dynamics and thermodynamics of large ash flows. *Bulletin of Volcanology* 58, 175–193.
- Camp, V.E., Ross, M.E., Hanson, W.E., 2003. Genesis of flood basalts and Basin and Range volcanic rocks from Steens Mountain to the Malheur River Gorge, Oregon. *Geological Society of America Bulletin* 115, 105–128.
- Carey, S.N., Sigurdsson, H., 1989. The intensity of plinian eruptions. *Bulletin of Volcanology* 51, 28–40.
- Cather, S.M., Dunbar, N.W., McDowell, F.W., McIntosh, W.C., Scholle, P.A., 2009. Climate forcing by iron fertilization from repeated ignimbrite eruptions: the icehouse-silicic large igneous province (SLIP) hypothesis. *Geosphere* 5, 315–324.
- Chenet, A.-L., Fluteau, F., Courtillot, V., 2008. Determination of rapid Deccan eruptions across the Cretaceous–Tertiary boundary using paleomagnetic secular variation: Results from a 1200-m-thick section in the Mahabaleshwar escarpment. *Journal of Geophysical Research* 113. doi:10.1029/2006JB004635.
- Chenet, A.-L., Courtillot, V., Fluteau, F., Gérard, M., Quidelleur, X., Khadri, S.F.R., Subbarao, K.V., Thordarson, T., 2009. Determination of rapid Deccan eruptions across the Cretaceous–Tertiary boundary using paleomagnetic secular variation: 2. Constraints from analysis of eight new sections and synthesis for a 3500-m-thick composite section. *Journal of Geophysical Research* 114, B06103. doi:10.1029/2008JB005644.
- Christiansen, R.L., 1979. Cooling units and composite sheets in relation to caldera structure. In: Chapin, C.E., Elston, W.E. (Eds.), *Ash-Flow Tuffs*: Geological Society of America Special Paper, 180, 29–42.
- Christiansen, R.L., 2001. The Quaternary and Pliocene Yellowstone Plateau Volcanic Field of Wyoming, Idaho, and Montana. USGS Professional Paper 729-G (120 pp.).
- Cleverly, R.W., 1977. The structural and magmatic evolution of the Lebombo Monocline, Southern Africa, with particular reference to Swaziland. Unpublished PhD thesis, University of Oxford, 316 pp.
- Cleverly, R.W., 1979. The volcanic geology of the Lebombo monocline in Swaziland. *Transactions Geological Society of South Africa* 82, 227–230.
- Coffin, M.F., Eldholm, O., 1994. Large igneous provinces: crustal structure, dimensions, and external consequences. *Reviews of Geophysics* 32, 1–36.
- Coffin, M.F., Eldholm, O., 2001. Large Igneous Provinces: progenitors of some ophiolites? In: Ernst, R.E., Buchan, K.L. (Eds.), *Mantle Plumes: Their Identification Through Time*: Geological Society of America Special Paper, vol. 352, pp. 59–70.
- Courtillot, V., 1999. *Evolutionary Catastrophes: The Science of Mass Extinction*. Cambridge University Press, Cambridge. (173 pp.).
- Courtillot, V.E., Renne, P.R., 2003. On the ages of flood basalt events. *Comptes Rendus Geoscience* 335, 113–140.
- Cox, K.G., 1980. A model for flood basalt volcanism. *Journal of Petrology* 21, 629–650.
- de Silva, S.L., 2009. Determining volumes of supereruptions – the pitfalls of “rules of thumb”. *Geological Society of America Abstracts with Programs* 41, 57.
- de Silva, S.L., Gosnold, W.D., 2007. Episodic construction of batholiths: insights from the spatiotemporal development of an ignimbrite flare-up. *Journal of Volcanology and Geothermal Research* 167, 320–335.
- Devey, C.W., Lightfoot, P.C., 1986. Volcanological and tectonic control of stratigraphy and structure in the western Deccan traps. *Bulletin of Volcanology* 48, 195–207.
- Duncan, A.R., Erlank, A.J., Marsh, J.S., 1984. Regional geochemistry of the Karoo igneous province. In: Erlank, A.J. (Ed.), *Petrogenesis of the volcanic rocks of the Karoo province*: Special Publication of the Geological Society of South Africa, 13, pp. 355–388.
- Elliot, D.H., Fleming, T.H., 2008. Physical volcanology and geological relationships of the Jurassic Ferrar Large Igneous Province, Antarctica. *Journal of Volcanology and Geothermal Research* 172, 20–37.
- Elliot, D.H., Fleming, T.H., Kyle, P.R., Foland, K.A., 1999. Long-distance transport of magmas in the Jurassic Ferrar Large Igneous Province, Antarctica. *Earth and Planetary Science Letters* 167, 89–104.
- Ernst, R.E., Buchan, K.L., 2001. Large mafic magmatic events through time and links to mantle-plume heads. In: Ernst, R.E., Buchan, K.L. (Eds.), *Mantle Plumes: Their Identification Through Time*: Geological Society of America Special Paper, vol. 352, pp. 483–575.
- Ewart, A., Milner, S.C., Armstrong, R.A., Duncan, A.R., 1998a. Etendeka volcanism of the Goboboseb Mountains and Messum Igneous complex Namibia. Part I: Geochemical evidence of Early Cretaceous Tristan plume melts and the role of crustal contamination in the Paraná–Etendeka CFB. *Journal of Petrology* 39, 191–225.
- Ewart, A., Milner, S.C., Armstrong, R.A., Duncan, A.R., 1998b. Etendeka volcanism of the Goboboseb Mountains and Messum Igneous Complex, Namibia Part II: Voluminous quartz latite volcanism of the Awahab magma system. *Journal of Petrology* 39, 227–253.
- Ewart, A., Milner, S.C., Duncan, A.R., Bailey, M., 2002. The Cretaceous Messum igneous complex, S.W. Etendeka, Namibia: reinterpretation in terms of a down-sag-cauldron subsidence model. *Journal of Volcanology and Geothermal Research* 114, 251–273.
- Ewart, A., Marsh, J.S., Milner, S.C., Duncan, A.R., Kamber, B.S., Armstrong, R.A., 2004a. Petrology and geochemistry of Early Cretaceous bimodal continental flood volcanism of the NW Etendeka, Namibia. Part 1: introduction, mafic lavas and re-evaluation of mantle source components. *Journal of Petrology* 45, 59–105.
- Ewart, A., Marsh, J.S., Milner, S.C., Duncan, A.R., Kamber, B.S., Armstrong, R.A., 2004b. Petrology and geochemistry of Early Cretaceous bimodal continental flood volcanism of the NW Etendeka, Namibia; Part 2 Characteristics and petrogenesis of the high-Ti latite and high-Ti and low-Ti voluminous quartz latite eruptives. *Journal of Petrology* 45, 107–138.
- Ferrari, L., Valencia-Moreno, M., Bryan, S.E., 2007. Magmatism and tectonics of the Sierra Madre Occidental and their relation to the evolution of the western margin of North America. *Geological Society of America, Special Papers* 442, 1–39.
- Ferrari, L., Ramos Rosique, A., Bryan, S.E., Rankin, A., 2009. Extensional tectonics triggering partial melting of shallow intrusions in the Bolaños graben, southern Sierra Madre Occidental, Mexico. *Geological Society of America Abstracts with Programs* 41, 56.
- Ferris, J., Johnson, A., Storey, B., 1998. Form and extent of the Dufek intrusion, Antarctica, from newly compiled aeromagnetic data. *Earth and Planetary Science Letters* 154, 185–202.
- Freundt, A., 1999. Formation of high-grade ignimbrites; II, A pyroclastic suspension current model with implications also for low-grade ignimbrites. *Bulletin of Volcanology* 60, 545–567.
- Gans, P.B., Mahood, G.A., Schermer, E.R., 1989. Synextensional magmatism in the Basin and Range Province; a case study from the eastern Great Basin. *Geological Society of America Special Paper* 233, 1–53.
- Garland, F.E., 1994. The Paraná rhyolites, southern Brazil: their petrogenetic relationship to the associated flood basalts. Unpublished PhD thesis, The Open University, 354 pp.
- Garland, F., Hawkesworth, C.J., Mantovani, M.S.M., 1995. Description and petrogenesis of the Paraná rhyolites, southern Brazil. *Journal of Petrology* 36, 1193–1227.
- Gorring, M., Naslund, H.R., 1995. Geochemical reversals within the lower 100 m of the Palisades sill, New Jersey. *Contributions to Mineralogy and Petrology* 119, 263–276.
- Green, J.C., Fitz, T.J., 1993. Extensive felsic lavas and rheoignimbrites in the Keweenaw Midcontinent Rift plateau volcanics, Minnesota: petrographic and field recognition. *Journal of Volcanology and Geothermal Research* 54, 177–196.
- Gunn, B.M., Warren, G., 1962. *Geology of Victoria Land between the Mawson and Mulock Glaciers, Antarctica*. New Zealand Geological Survey Bulletin 71, 1–157.
- Heister, L.E., O'Day, P.A., Brooks, C.K., Neuhoff, P.S., Bird, D.K., 2001. Pyroclastic deposits within the East Greenland Tertiary flood basalts. *Journal of the Geological Society of London* 158, 269–284.
- Hildreth, W., 1981. Gradients in silicic magma chambers: implications for lithospheric magmatism. *Journal of Geophysical Research* 86 (B11), 10,153–10,192.
- Hooper, P.R., 1997. The Columbia River flood basalt province: current status. In: Mahoney, J.J., Coffin, M.F. (Eds.), *Large Igneous Provinces: Continental, Oceanic, and Planetary Flood Volcanism*: American Geophysical Union, Geophysical Monograph, 100, pp. 1–27.
- Hooper, P.R., Camp, V.E., Reidel, S.P., Ross, M.E., 2007. The Columbia River Basalts and their relationship to the Yellowstone hotspot and Basin and Range extension. In: Foulger, G.R., Jurdy, J.M. (Eds.), *Plumes, Plates, and Planetary Processes*: Geological Society of America Special Paper, 430, pp. 635–668.
- Husch, J.M., 1990. Palisades sill: origin of the olivine zone by separate magmatic injection rather than gravity settling. *Geology* 18, 699–702.
- Jay, A.E., Widdowson, M., 2006. Stratigraphy, structure and volcanology of the SE Deccan continental flood basalt province: implications for eruptive extent and volumes. *Journal of the Geological Society* 165, 177–188.
- Jay, A.E., Mac Niocaill, C., Widdowson, M., Self, S., Turner, W., 2009. New palaeomagnetic data from the Mahabaleshwar Plateau, Deccan Flood Basalt Province, India: implications for the volcanostratigraphic architecture of continental flood basalt provinces. *Journal of the Geological Society* 166, 13–24.
- Jerram, D.A., 2002. Volcanology and facies architecture of flood basalts. In: Menzies, M. A., Klemperer, S.L., Ebinger, C.J., Baker, J. (Eds.), *Magmatic Rifted Margins*: Geological Society of America Special Paper, 362, pp. 119–132.
- Jerram, D.A., Widdowson, M., 2005. The anatomy of Continental Flood Basalt Provinces: geological constraints on the process and products of flood volcanism. *Lithos* 79, 385–405.
- Jerram, D.A., Mountney, N., Holzförster, F., Stollhofen, H., 1999. Stratigraphic relationships in the Etendeka Group in the Huab Basin, NW Namibia: Understanding the onset of flood volcanism. *Journal of Geodynamics* 28, 393–418.
- Jolley, D.W., Widdowson, M., Self, S., 2008. Volcanogenic nutrient fluxes and plant ecosystems in large igneous provinces: an example from the Columbia River Basalt Group. *Journal of the Geological Society, London* 165, 955–966.
- Kelley, S., 2007. Geochronology of LIPs, terrestrial impact craters and their relationship to mass extinctions on Earth. *Journal of the Geological Society of London* 164, 923–936.
- Kerr, A.C., Mahoney, J.J., 2007. Oceanic plateaus: problematic plumes, potential paradigms. *Chemical Geology* 241, 332–353.
- Keszthelyi, L., 2002. Classification of mafic lava flows from ODP Leg 183. *Proceedings of the Ocean Drilling Program, Scientific Results*, 183 ([http://www.odp.tamu.edu/publications/183-SR/012/012.htm]).
- Keszthelyi, L., Self, S., 1998. Some physical requirements for the emplacement of long basaltic lava flows. *Journal of Geophysical Research* 103 (b11), 27447–27464.
- Keszthelyi, L., Thordarson, T., McEwen, A., Haack, H., Guilbaud, M.-N., Self, S., Rossi, M.J., 2004. Icelandic analogs to Martian flood lavas. *Geochemistry, Geophysics, Geosystems* 5 (G3), Q11014. doi:10.1029/2004GC000758.
- Keszthelyi, L., Self, S., Thordarson, T., 2006. Flood lavas on Earth, Io and Mars. *Journal of the Geological Society of London* 163, 253–264.
- Kirstein, L.A., Peate, D.W., Hawkesworth, C.J., Turner, S.P., Harris, C., Mantovani, M.S.M., 2000. Early Cretaceous basaltic and rhyolitic magmatism in southern Uruguay associated with the opening of the South Atlantic. *Journal of Petrology* 41, 1413–1438.
- Kirstein, L.A., Hawkesworth, C.J., Garland, F., 2001. Silicic lavas versus rheomorphic ignimbrites: A chemical distinction? *Contributions to Mineralogy and Petrology* 142, 309–322.
- Koyaguchi, T., 1996. Volume estimation of tephra-fall deposits from the June 15, 1991 eruption of Mount Pinatubo by theoretical and geological methods. In: Newhall, C.G., Punongbayan, R.S. (Eds.), *Fire and Mud: Eruptions and Lahars of Mount Pinatubo, Philippines*. University of Washington Press, Seattle, pp. 583–600.
- Koyaguchi, T., Tokuno, M., 1993. Origin of the giant eruption cloud of Pinatubo, June 15, 1991. *Journal of Volcanology and Geothermal Research* 55, 85–96.
- Landon, R.D., Long, P.E., 1989. Detailed stratigraphy of the N₂ Grande Ronde Basalt, Columbia River Basalt Group, in the central Columbia Plateau. In: Reidel, S.P., Hooper, P.R. (Eds.), *Volcanism and tectonism in the Columbia River flood-basalt province*: Geological Society of America Special Paper, vol. 239, pp. 55–66.

- Larsen, L.M., Fitton, J.G., Pedersen, A.K., 2003. Paleogene volcanic ash layers in the Danish basin: compositions and source areas in the North Atlantic Igneous Province. *Lithos* 71, 47–80.
- Larsen, L.M., Pedersen, A.K., Pedersen, G.K., 2006. A subaqueous rootless cone field at Niuluut, Disko, Paleocene of West Greenland. *Lithos* 92, 20–32.
- Lipman, P.W., 1997. Chasing the volcano. *Earth* 33–39.
- Lipman, P.W., Steven, T.A., Mehnert, H.H., 1970. Volcanic history of the San Juan Mountains, Colorado, as indicated by Potassium–Argon dating. *Geological Society of America Bulletin* 81, 2329–2352.
- Mahoney, J.J., Saunders, A.D., Storey, M., Randriamanantenaso, A., 2008. Geochemistry of the Volcan de l'Androy basalt–rhyolite complex, Madagascar Cretaceous Igneous Province. *Journal of Petrology* 49, 1069–1096.
- Mangan, M.T., Wright, T.L., Swanson, D.A., Byerly, G.R., 1986. Regional correlation of Grande Ronde flows, Columbia River basalt group, Washington, Oregon and Idaho. *Geological Society of America Bulletin* 97, 1300–1318.
- Marsh, J.S., Ewart, A., Milner, S.C., Duncan, A.R., Miller, R. McG., 2001. The Etendeka igneous province; magma types and their stratigraphic distribution with implications for the evolution of the Paraná–Etendeka flood basalt province. *Bulletin of Volcanology* 62, 464–486.
- Mason, B.G., Pyle, D.M., Oppenheimer, C., 2004. The size and frequency of the largest explosive eruptions on Earth. *Bulletin of Volcanology* 66, 735–748.
- Maughan, L.L., Christiansen, E.H., Best, M.G., Gromme, C.S., Deino, A.L., Tingey, D.G., 2002. The Oligocene Lund Tuff, Great Basin, USA: a very large volume monotonous intermediate. *Journal of Volcanology and Geothermal Research* 113, 129–157.
- Mawby, M., 2008. Out of Africa: Explosive volcanism in the Paraná–Etendeka Province. Namibia. *Geoscientist* 18.10 October 2008. The Geological Society.
- Mawby, M.R., Bryan, S.E., Jerram, D.A., Davidson, J.P., 2006. How are 'Super' eruptions preserved in the past? Volcanological features of large volume silicic eruptions of the Paraná–Etendeka. *EOS. Transactions of the American Geophysical Union* 87 (52) (Fall Meeting Supplement, Abstract V33-0683).
- McPhie, J., Della Pasqua, F., Allen, S.R., Lackie, M., 2008. Extreme effusive eruptions: palaeoflow data on an extensive felsic lava in the Mesoproterozoic Gawler Range Volcanics. *Journal of Volcanology and Geothermal Research* 172, 148–161.
- Melluso, L., Beccaluva, L., Brotzu, P., Gregnanin, A., Gupta, A.K., Morbidelli, L., Traversa, G., 1995. Constraints on the mantle sources of the Deccan Traps from the petrology and geochemistry of the basalts of Gujarat State (western India). *Journal of Petrology* 36, 1393–1432.
- Miller, C.F., Wark, D.A., 2008. Supervolcanoes and their supereruptions. *Elements* 4, 11–16.
- Miller, J.A., Harris, C., 2007. Petrogenesis of the Swaziland and northern Natal rhyolites of the Lebombo rifted volcanic margin, South East Africa. *Journal of Petrology* 48, 185–218.
- Milner, S.C., 1988. The geology and geochemistry of the Etendeka Formation quartz latites, Namibia. Unpublished Ph.D. thesis, University of Cape Town, 263 pp.
- Milner, S.C., Duncan, A.R., 1987. Geochemical characterization of quartz latite units in the Etendeka Formation. *Communications of the Geological Survey of South West Africa/Namibia* 3, 83–90.
- Milner, S.C., Ewart, A., 1989. The geology of the Goboboseb Mountains volcanics and their relationship to the Messum Complex. *Communications of the Geological Survey of Namibia* 5, 31–40.
- Milner, S.C., Duncan, A.R., Ewart, A., 1992. Quartz latite rheognimbrite flows of the Etendeka Formation, north-western Namibia. *Bulletin of Volcanology* 54, 200–219.
- Milner, S.C., Duncan, A.R., Whittingham, A.M., Ewart, A., 1995. Trans-Atlantic correlation of eruptive sequences and individual silicic volcanic units within the Paraná–Etendeka igneous province. *Journal of Volcanology and Geothermal Research* 69, 137–157.
- Moore, C.L., 1991. The distal terrestrial record of explosive rhyolitic volcanism: an example from Auckland, New Zealand. *Sedimentary Geology* 74, 25–38.
- Nardy, A.J.R., Machado, F.B., Farias de Oliveira, M.A., 2008. As rochas vulcânicas mesozóicas ácidas da Bacia do Paraná: litoestratigrafia e considerações geoquímico-estratigráficas. *Revista Brasileira de Geociências* 38, 178–195.
- Pattan, J.N., Pearce, N.J.G., Banakar, V.K., Parthiban, G., 2002. Origin of ash in the Central Indian Ocean Basin and its implication for the volume estimate of the 74,000 year BP Youngest Toba eruption. *Current Science* 83, 889–893.
- Peate, D.W., 1997. The Paraná–Etendeka province. In: Mahoney, J.J., Coffin, M. (Eds.), *Large Igneous Provinces: Continental, Oceanic, and Planetary Volcanism: Geophysical Monograph Series*, v. 100. American Geophysical Union, pp. 217–245.
- Peate, D.W., 2009. Global dispersal of Pb by large-volume silicic eruptions in the Paraná–Etendeka large igneous province. *Geology* 37, 1071–1074.
- Peate, D.W., Hawkesworth, C.J., 1996. Lithospheric to asthenospheric transition in Low-Ti flood basalts from the southern Paraná, Brazil. *Chemical Geology* 127, 1–24.
- Peate, D.W., Hawkesworth, C.J., Mantovani, M.S.M., 1992. Chemical stratigraphy of the Paraná lavas (South America): classification of magma types and their spatial distribution. *Bulletin of Volcanology* 55, 119–139.
- Peate, D.W., Hawkesworth, C.J., Mantovani, M.S.M., Rogers, N.W., Turner, S.P., 1999. Petrogenesis and stratigraphy of the high Ti/Y Rubric magma type in the Paraná flood basalt province and implications for the nature of 'Dupal'-type mantle in the South Atlantic region. *Journal of Petrology* 40, 451–473.
- Piccirillo, E.M., Raposo, M.I.B., Melfi, A.J., Comin-Chiaromonte, P., Bellieni, G., Cordani, U. G., Kawashita, K., 1987. Bimodal fissural volcanic suites from the Paraná basin (Brazil): K–Ar age, Sr isotopes and geochemistry. *Geochim Brasiliensis* 1, 53–69.
- Prokoph, A., Ernst, R.E., Buchan, K.L., 2004. Time-series analysis of Large Igneous Provinces: 3500 Ma to Present. *Journal of Geology* 112, 1–22.
- Puffer, J.H., Block, K.A., Steiner, J.C., 2009. Transmission of flood basalts through a shallow crustal sill and the correlation of sill layers with extrusive flows: the Palisades intrusive system and the basalts of the Newark Basin, New Jersey, U.S.A. *The Journal of Geology* 117, 139–155.
- Pyle, D.M., 1995. Mass and energy budgets of explosive volcanic eruptions. *Geophysical Research Letters* 5, 563–566.
- Pyle, D.M., 2000. The sizes of volcanic eruptions. In: Sigurdsson, H., Houghton, B., McNutt, S.R., Rymer, H., Stix, J. (Eds.), *Encyclopedia of Volcanoes*. Academic Press, London, UK, pp. 263–269.
- Ramos, F.C., Wolff, J.A., Tollstrup, D.L., 2005. Sr isotope disequilibrium in Columbia River flood basalts: Evidence for rapid, shallow-level open-system processes. *Geology* 33, 457–460.
- Rampino, M.R., Stothers, R.B., 1988. Flood basalt volcanism during the past 250 million years. *Science* 241, 663–668.
- Reidel, S.P., 1983. Stratigraphy and petrogenesis of the Grande Ronde Basalt from the deep canyon country of Washington, Oregon and Idaho. *Geological Society of America Bulletin* 94, 519–542.
- Reidel, S.P., 2005. A lava flow without a source: The Cohasset flow and its compositional components, Sentinel Bluffs Member, Columbia River Basalt Group. *Journal of Geology* 113, 1–21.
- Reidel, S.P., Tolan, T.L., 1992. Eruption and emplacement of flood basalt; an example from the large-volume Teepee Butte Member, Columbia River Basalt Group. *Geological Society of America Bulletin* 104, 1650–1671.
- Reidel, S.P., Tolan, T.L., Hooper, P.R., Beeson, M.H., Fecht, K.R., Bentley, R.D., Anderson, J.L., 1989. The Grande Ronde Basalt, Columbia River Basalt Group; stratigraphic descriptions and correlations in Washington, Oregon, and Idaho. *Geological Society of America Special Paper* 239, 21–53.
- Reidel, S.P., Campbell, N.P., Fecht, K.R., Lindsey, K.A., 1994. Late Cenozoic structure and stratigraphy of south-central Washington. In: Lasmanis, R., Cheney, E.S. (Eds.), *Regional geology of Washington State: Washington Division of Geology and Earth Resources Bulletin*, vol. 80, pp. 159–180.
- Reiners, P.W., 2002. Temporal-compositional trends in intraplate basalt eruptions: Implications for mantle heterogeneity and melting processes. *Geochemistry, Geophysics, Geosystems* 3 (2) (paper 2001GC000250).
- Renne, P.R., Glen, J.M., Milner, S.C., Duncan, A.R., 1996. Age of Etendeka flood volcanism and associated intrusions in southwestern Africa. *Geology* 24, 659–662.
- Rodriguez Durand, S., Sen, G., 2004. Preruption history of the Grande Ronde Formation lavas Columbia River Basalt Group. *American northwest: Evidence from phenocrysts*. *Geology* 32, 293–296.
- Rose, W.I., Chesner, C.A., 1987. Dispersal of ash in the great Toba eruption, 75 ka. *Geology* 15, 913–917.
- Ross, P.-S., Ukstins Peate, I., McClintock, M.K., Xu, Y.G., Skilling, I.P., White, J.D.L., Houghton, B.F., 2005. Mafic volcanoclastic deposits in flood basalt provinces: a review. *Journal of Volcanology and Geothermal Research* 145, 281–314.
- Self, S., 1992. Krakatau revisited: the course of events and interpretation of the 1883 eruption. *GeoJournal* 28, 109–121.
- Self, S., 2006. The effects and consequences of very large explosive volcanic eruptions. *Philosophical Transactions of the Royal Society A364*, 2073–2097.
- Self, S., Thordarson, T., Keszthelyi, L., Walker, G.P.L., Hon, K., Murphy, M.T., Long, P., Finnemore, S., 1996. A new model for the emplacement of Columbia River basalts as large, inflated pahoehoe lava flow fields. *Geophysical Research Letters* 23, 2689–2692.
- Self, S., Thordarson, T., Keszthelyi, L., 1997. Emplacement of continental flood basalt lava flows. In: Mahoney, J.J., Coffin, M. (Eds.), *Large Igneous Provinces: Continental, Oceanic, and Planetary Volcanism: Geophysical Monograph Series*, 100. American Geophysical Union, pp. 381–410.
- Self, S., Keszthelyi, L., Thordarson, T., 1998. The importance of pahoehoe. *Annual Review of Earth and Planetary Sciences* 26, 81–110.
- Self, S., Thordarson, T., Widdowson, M., 2005. Gas fluxes from flood basalt eruptions. *Elements* 1, 283–287.
- Self, S., Widdowson, M., Thordarson, T., Jay, A.E., 2006. Volatile fluxes during flood basalt eruptions and potential effects on the global environment: a Deccan perspective. *Earth and Planetary Science Letters* 248, 518–532.
- Self, S., Jay, A.E., Widdowson, M., Keszthelyi, L.P., 2008. Correlation of the Deccan and Rajahmundry Trap lavas: Are these the longest and largest lava flows on Earth? *Journal of Volcanology and Geothermal Research* 172, 3–19.
- Shaw, H.R., Swanson, D.A., 1970. Eruption and flow rates of flood basalts. In: Gilmour, E.H., Stradling, D.F. (Eds.), *Proceedings of the second Columbia River Basalt Symposium: Cheney*. Eastern Washington State College Press, pp. 271–299.
- Sparks, R.S.J., 1986. The dimensions and dynamics of volcanic eruption columns. *Bulletin of Volcanology* 48, 3–15.
- Sparks, R.S.J., Walker, G.P.L., 1977. The significance of vitric-enriched air-fall ashes associated with crystal-enriched ignimbrites. *Journal of Volcanology and Geothermal Research* 2, 329–341.
- Sparks, R.S.J., Self, S., working group, 2005. *Super-eruptions: global effects and future threats*. Rep Geol Soc London Working Group (2nd ed), Geological Society, London, United Kingdom, p. 24.
- Stephenson, P.J., Burch-Johnston, A.T., Stanton, D., Whitehead, P.W., 1998. Three long lava flows in north Queensland. *Journal of Geophysical Research* 103 (B11), 27,259–27,370.
- Storey, M., Duncan, R.A., Tegner, C., 2007. Timing and duration of volcanism in the North Atlantic Igneous Province: Implications for geodynamics and links to the Iceland hotspot. *Chemical Geology* 241, 264–281.
- Straub, S.M., Schmincke, H.U., 1998. Evaluating the tephra input into Pacific Ocean sediments: distribution in space and time. *Geologische Rundschau* 87, 461–476.
- Streck, M., Grunder, A., 2008. Phenocryst-poor rhyolites of bimodal, tholeiitic provinces: the Rattlesnake Tuff and implications for mush extraction models. *Bulletin of Volcanology* 70, 385–401.

- Swanson, D.A., Wright, T.L., Helz, R.T., 1975. Linear vent systems and estimated rates of magma production and eruption for the Yakima Basalt on the Columbia Plateau. *American Journal of Science* 275, 877–905.
- Swanson, E.R., Kempton, K., McDowell, F.W., McIntosh, W.C., 2006. Major ignimbrites and volcanic centers of the Copper Canyon area: A view into the core of Mexico's Sierra Madre Occidental. *Geosphere* 2, 25–141.
- Taylor, B., 2006. The single largest oceanic plateau: Ontong Java-Manihiki-Hikurangi. *Earth and Planetary Science Letters* 241, 372–380.
- Thordarson, T., Self, S., 1993. The Laki (Skaftar Fires) and Grimsvotn eruptions in 1783–1785. *Bulletin of Volcanology* 55, 233–263. doi:10.1007/BF00624353.
- Thordarson, T., Self, S., 1996. Sulfur, chlorine and fluorine degassing and atmospheric loading by the Roza eruption, Columbia River Basalt Group, Washington, USA. *Journal of Volcanology and Geothermal Research* 74, 49–73. doi:10.1016/S0377-0273(96)00054-6.
- Thordarson, T., Self, S., 1998. The Rosa Member, Columbia River Basalt Group: A gigantic pahoehoe lava flow field formed by endogenous processes? *Journal of Geophysical Research* 103 (no. B11), 27,411–27,445.
- Thordarson, T., Rampino, M., Keszthelyi, L., Self, S., 2009. Effects of megascale eruptions on Earth and Mars. In: Chapman, M.G., Keszthelyi, L.P., (Eds.), *Preservation of random megascale events on Mars and Earth: Influence on geologic history: Geological Society of America Special Paper* 453, 37–55.
- Tolan, T.L., Reidel, S.P., Beeson, M.H., Anderson, J.L., Fecht, K.R., Swanson, D., 1989. In: Reidel, S.P., Hooper, P.R. (Eds.), *Revisions to the estimates of the areal extent and volume of the Columbia River Flood Basalt Province: In Reidel, S.P., Hooper, P.R. (Eds.), Volcanism and tectonism in the Columbia River flood-basalt province. Special Paper of the Geological Society of America*, 239, pp. 1–20.
- Trendall, A., 1995. The Woongara Rhyolite – a giant lava-like felsic sheet in the Hamersley Basin of Western Australia. *Geological Survey of Western Australia Report* 42 (70 p.).
- Twist, D., French, B.M., 1983. Voluminous acid volcanism in the Bushveld Complex: a review of the Rooiberg Felsite. *Bulletin of Volcanology* 46, 225–242.
- Ukstins Peate, I., Bryan, S.E., 2008. Re-evaluating plume-induced uplift in the Emeishan large igneous province. *Nature Geoscience* 1, 625–629.
- Ukstins Peate, I., Baker, J.A., Kent, A.J.R., Al-Kadasi, M., Al-Subbary, A., Ayalew, D., Menzies, M., 2003. Correlation of Indian Ocean tephra to individual Oligocene silicic eruptions from Afro-Arabian flood volcanism. *Earth and Planetary Science Letters* 211, 311–327.
- Ukstins Peate, I., Baker, J.A., Al-Kadasi, M., Al-Subbary, A., Knight, K.B., Riisager, P., Thirlwall, M.F., Peate, D.W., Renne, P.R., Menzies, M.A., 2005. Volcanic stratigraphy of large-volume silicic pyroclastic eruptions during Oligocene Afro-Arabian flood volcanism in Yemen. *Bulletin of Volcanology* 68, 135–156.
- Ukstins Peate, I., Kent, A.J.R., Baker, J.A., Menzies, M.A., 2008. Extreme geochemical heterogeneity in Afro-Arabian Oligocene tephras: Preserving fractional crystallization and mafic recharge processes in large-volume silicic magma chambers. *Lithos* 102, 260–278.
- Vogel, T.A., 1982. Magma mixing in the acidic-basic complex of Ardnamurchan: implications on the evolution of shallow magma chambers. *Contributions to Mineralogy and Petrology* 79, 411–423.
- Walker, G.P.L., 1972. Compound and simple lava flows and flood basalts. *Bulletin of Volcanology* 35, 579–590.
- Walker, G.P.L., 1981. Plinian eruptions and their products. *Bulletin of Volcanology* 44, 223–240.
- Waters, A.C., 1960. Determining the direction of flow in basalts. *American Journal of Science* 258-A, 350–366.
- White, S.M., Crisp, J.A., Spera, F.A., 2006. Long-term volumetric eruption rates and magma budgets. *Geochemistry, Geophysics, Geosystems* 7. doi:10.1029/2005GC001002.
- White, J.D.L., Bryan, S.E., Ross, P.-S., Self, S., Thordarson, T., 2009. Physical volcanology of continental large igneous provinces: update and review. In: Thordarson, T., Self, S., Larsen, G., Rowland, S.K., Hoskuldsson, A. (Eds.), *Studies in Volcanology: The Legacy of George Walker. Special Publications of IAVCEI*, 2. Geological Society, London, pp. 291–321.
- Whittingham, A.M. 1991. Stratigraphy and petrogenesis of the volcanic formations associated with the opening of the South Atlantic, Southern Brazil. Unpublished Ph.D. thesis, University of Oxford, 162 pp.
- Wignall, P.B., 2001. Large igneous provinces and mass extinctions. *Earth Science Reviews* 53, 1–33.
- Wignall, P.B., 2005. The link between Large Igneous Province eruptions and mass extinctions. *Elements* 1, 293–297.
- Wilson, C.J.N., 2001. The 26.5 ka Oruanui eruption, New Zealand: an introduction and overview. *Journal of Volcanology and Geothermal Research* 112, 133–174.
- Wilson, C.J.N., 2008. Supereruptions and supervolcanoes: Processes and products. *Elements* 4, 29–34.
- Wilson, C.J.N., Hildreth, W., 1997. The Bishop Tuff: new insights from eruptive stratigraphy. *Journal of Geology* 105, 407–439.
- Wilson, L., Walker, G.P.L., 1987. Explosive volcanic eruptions – VI. Ejecta dispersal in plinian eruptions: the control of eruption conditions and atmospheric properties. *Geophysical Journal of the Royal Astronomical Society* 89, 657–679.
- Wilson, L., Sparks, R.S.J., Huang, T.C., Watkins, N.D., 1978. The control of volcanic column heights by eruption energetics and dynamics. *Journal of Geophysical Research* 83, 1829–1836.
- Wilson, L., Sparks, R.S.J., Walker, G.P.L., 1980. Explosive volcanic eruptions: IV. The control of magma properties and conduit geometry on eruption column behaviour. *Geophysical Journal of the Royal Astronomical Society* 63, 117–148.
- Woods, A.W., 1995. The dynamics of explosive volcanic eruptions. *Reviews of Geophysics* 33, 495–530.
- Woods, A.W., Wohletz, K., 1991. Dimensions and dynamics of cognimbrite eruption columns. *Nature* 350, 225–227.